Scaled free energies, power-law potentials, strain pseudospins and quasi-universality for first-order structural transitions

S.R. Shenoy*, T. Lookman†, and A. Saxena†
*School of Physics, University of Hyderabad, Hyderabad 500046, India,
*International Centre for Theoretical Physics, Trieste 34014, Italy
†Theoretical Division, Los Alamos National Laboratory, Los Alamos, NM 87545, USA
(Dated: November 1, 2010)

We consider ferroelastic first-order phase transitions with N_{OP} order-parameter strains entering Landau free energies as invariant polynomials, that have N_V structural-variant Landau minima. The total free energy includes (seemingly innocuous) harmonic terms, in the $n = 6 - N_{OP}$ *non*-order-parameter strains. Four 3D transitions are considered, tetragonal/orthorhombic, cubic/tetragonal, cubic/trigonal and cubic/orthorhombic unit-cell distortions, with respectively, $N_{OP} = 1, 2, 3$ and 2; and $N_V = 2, 3, 4$ and 6. Five 2D transitions are also considered, as simpler examples. Following Barsch and Krumhansl, we scale the free energy to absorb most material-dependent elastic coefficients into an overall prefactor, by scaling in an overall elastic energy density; a dimensionless temperature variable; and the spontaneous-strain magnitude at transition $\lambda << 1$. To leading order in λ the scaled Landau minima become material-independent, in a kind of 'quasi-universality'. The scaled minima in N_{OP}-dimensional order-parameter space, fall at the centre and at the N_V corners, of a transition-specific polyhedron inscribed in a sphere, whose radius is unity at transition. The 'polyhedra' for the four 3D transitions are respectively, a line, a triangle, a tetrahedron, and a hexagon. We minimize the n terms harmonic in the non-order-parameter strains, by substituting solutions of the 'no dislocation' St Venant compatibility constraints, and explicitly obtain powerlaw anisotropic, order-parameter interactions, for all transitions. In a reduced discrete-variable description, the competing minima of the Landau free energies induce unit-magnitude pseudospin vectors, with $N_V + 1$ values, pointing to the polyhedra corners and the (zero-value) center. The total scaled free energies then become $\mathbb{Z}_{N_V+1}$ clock-like pseudospin hamiltonians, with temperature-dependent local Landau terms, nearest-neighbor Ginzburg couplings, and powerlaw St Venant interactions that drive the elastic domain-wall texturing. The scaled free energies can be used in relaxational or underdamped dynamic simulations, to study ferroelastic strain textures and their dynamical evolution pathways. The pseudospin models can similarly be studied via local meanfield treatments, and Monte Carlo simulations.

I. INTRODUCTION

Although first order phase transitions predominate in nature, second-order transitions have attracted much theoretical attention, because of the taxonomically simplifying concept of 'universality classes'[1]. Diverse materials in the same universality class have common critical exponent values as a scaled temperature $T/T_c \to 1$, that depend only on the dimensionality d of coordinate space; the number N_{OP} of order parameter components; and the number N_V of degenerate energy minima or 'variants'. Spin models are prototypical, with $d = 2$, $N_{OP} = 1$, $N_V = 2$ for a 2D Ising model. The symmetry-breaking transition is signalled by spontaneous nonzero averages of a spin component, as one of the degenerate-minima variants in order parameter (*OP*) space is picked out. First-order transitions by contrast, seem to be inherently material specific, as they lack a divergent length scale to induce universality, by rendering irrelevant the finite-scale material parameters. On the other hand, precisely because critical fluctuations are unimportant, an approach focusing on free energy minima is more reliable. If the free energies could be scaled to make at least these minima independent of the material coefficients, one would have a kind of 'quasi-universality' for first-order transitions.

Ferroelastic, displacive structural transformations[2–6] as in the austenite/martensite transition are (mostly) first order, symmetry lowering transitions, with the discrete symmetries of high/low temperature lattices often having a group/subgroup relationship. Lattices in d dimensions have $d(d+1)/2$ Cartesian strain-tensor components, whose linear combinations are the same number of physical strains, of which N_{OP} are the order parameters. The Landau variational free energies are sums of high-order polynomial invariants in the OP, with many material-specific anharmonic elastic coefficients[6,7], that take effort to extract from experiments. With a single high temperature zero-strain state, and N_V other structural variants apppearing as temperature is lowered, there are $N_V + 1$ degenerate Landau minima at the first-order transition temperature. Twinning, or spatial coexistence of competing structures separated by oriented domain walls, is common[2,8]. The orientation comes from long-range elastic forces[8] or powerlaw anisotropic interactions[11–17] between the N_{OP} order parameters, that are present but hidden, in the conventional displacement representation. As will be seen, these effective interactions[11], arise from a *constrained* minimization of free energy harmonic terms in the $n = d(d+1)/2 - N_{OP}$ non-order-parameter strains, subject to St. Venant compatibility conditions[9,10].

Barsch and Krumhansl (BK)[18] have scaled the Landau free energy of a 2D square/rectangle transition, and the 3D cubic/tetragonal transition using three scaling parameters, to a dimensionless form that is internally independent of elastic coefficients. A conceptually important dimensionless temperature variable $\tau(T) \equiv (T - T_c)/(T_0 - T_c)$ can be introduced, that absorbs elastic coefficients of the quadratic term in the OP-strain magnitude. It is unity $\tau(T_0) = 1$ at the first order transition temperature $T = T_0$; while it vanishes $\tau(T_c) = 0$ at the lower spinodal T_c.

In this paper, we generalize this BK procedure for the Landau free energies of four 3D and five 2D transitions, that can have $N_{OP} = 1, 2, 3$ order parameters, and $N_V = 2, 3, 4, 6$ variants, to absorb the (often unknown) material coefficients[6,7], into an overall energy prefactor. The four $3D$ transitions are tetragonal to orthorhombic, cubic to tetragonal, cubic to trigonal; and cubic to orthorhombic, with their number of unscaled material coefficients respectively $N_{mat} = 3, 3, 4$ and 6. The 3D transitions we have chosen are relevant for functional materials : tetragonal/ orthorhombic (as for high-temperature superconductors such as YBCO); cubic/ tetragonal (as for shape memory alloys such as FePd); cubic/orthorhombic (as for ferroelectrics such as $BaTiO$); and cubic/trigonal (as for CMR oxides such as $LaSrMnO$). We show that, apart from the overall energy-density coefficient, the scaled free energies evaluated at the $N_V + 1$ minima are material-independent in the first three 3D cases, and weakly dependent on a single material parameter in the cubic-orthorhombic case. The minima fall at the center and corners of a transition-specific polyhedron inscribed in a sphere, of unit radius at transition. The 'polyhedron' for $N_{OP} = 1, 2$ or 3 can be a line, a triangle, a hexagon or a tetrahedron. We evaluate the St Venant compatibility potentials through their $N_{OP} \times N_{OP}$ matrix kernels, for all the nine transitions using a constraint substitution method, that is more direct than a Lagrange multiplier[11] method. The scaled total free energies can be used in over-damped, or under-damped OP strain dynamics (that includes Langevin noise terms with powerlaw anisotropic spatial correlations)[12,13]. In a reduced, discrete-variable description that retains only the Landau minima, the total scaled free energies induce clock[19] like '$\mathbb{Z}_{N_V+1}$' hamiltonians in terms of unit-magnitude, N_{OP}-dimensional vectors, pointing to $N_V + 1$ values. The hamiltonians are bilinear in the pseudospins, with (temperature-dependent) quadratic on-site contributions from the Landau term; nearest-neighbor ferromagnetic couplings from the Ginzburg term; and powerlaw anisotropic interaction potentials from the St Venant term. The pseudospin hamiltonians can be used for local meanfield treatments, and Monte Carlo simulations, of ferroelastic textures. The models are also be relevant for complex functional materials, with lattice strains coupled to intracell charge, spin and orbitals[17].

In more detail, the transition-specific scaling procedure involves a choice of three scaling parameters: a typical spontaneous strain magnitude λ that is small; a typical elastic energy density E_0; and a (Landau) first-order transition temperature T_0 chosen such that the scaled BK temperature variable $\tau(T_0) = 1$, and the scaled OP magnitude is unity at transition. The smallness of $\lambda << 1$ justifies a finite-sum truncation of the expansion in invariants; and a neglect of geometric nonlinearities inside the Lagrangian strains, as a perturbative first approximation. Working to leading order in λ, yields a 'quasi-universal' scaled Landau term that has an overall, material-dependent energy density E_0, as mentioned. The total free energy has Ginzburg and St Venant terms that determine elastic domain-wall texturing, and carry (two) material-dependent coefficients. Elastic pseudospin models in the context of martensites have been considered by several groups[20–25], but the models obtained here are explicitly induced by scaled free energies.

In Sec. II we set up the general BK scaling procedure for 2D and 3D free energies. We then consider transitions in increasing number of variants, $N_V = 2, 3, 4, 6$. In Sec. III we consider two-variant, single order parameter $N_V = 2, N_{OP} = 1$ cases, namely the 3D tetragonal/orthorhombic transition; and in 2D the square/rectangle or square/ rhombus; and rectangle/oblique-polygon transitions. Section IV considers cases with $N_V = 3$ and $N_{OP} = 2$, namely the 3D cubic/ tetragonal, and 2D triangle/ centered- rectangle transitions. Section V considers $N_V = 4$ cases: the 3D cubic/ trigonal ($N_{OP} = 3$), and 2D square/ oblique ($N_{OP} = 2$). Section VI presents the $N_V = 6, N_{OP} = 2$ case of 3D cubic/ orthorhombic and 2D triangle/ oblique transitions. Section VII obtains the reduced pseudospin hamiltonians, for all the transitions. Section VIII outlines possible simulation approaches, while the last Section IX is a summary. An overview in Table I collects the generic numbers of the scaled Landau free energies, common to all materials with a given transition in the same quasi-universality class. The Appendix derives compatibility kernels for the four 3D and five 2D transitions considered, through the direct substitution method, contributing to a 'library of kernels' for use in simulations.

II. SCALING PROCEDURE

Here (A) we define elastic variables, and (B) state the general scaling procedure.

A. Distortion and strains

The distortion tensor[9] $D_{\mu\nu}$ can be defined in terms of gradients of the displacement vector $\vec{u}(\vec{r})$ of points in a continuum medium, by

$$D_{\mu\nu}(\vec{r}) = \partial u_\mu(\vec{r})/\partial r_\nu, \quad (2.1a)$$

where μ, ν run over x, y, z; or in Fourier space,

$$D_{\mu\nu}(\vec{k}) = i u_\mu(\vec{k}) k_\nu. \quad (2.1b)$$

The $\mathbf{D}$ tensor is a sum $\mathbf{D} \equiv \mathbf{e} + \mathbf{w}$ of a symmetrized ($\mathbf{e}$) and antisymmetrized ($\mathbf{w}$) distortion (or local rotation) tensor. With 'T' a transpose,

$$\mathbf{e}(\vec{r}) \equiv \frac{1}{2}[\mathbf{D} + \mathbf{D}^T]; \;\; \mathbf{w}(\vec{r}) \equiv \frac{1}{2}[\mathbf{D} - \mathbf{D}^T]. \quad (2.2)$$

We will refer to the symmetrized distortion tensor $e_{\mu\nu}$ as the 'strain' tensor, and take it as the working variable, in a *strain representation*. It is distinct from the 'Lagrangian-strain' $E_{\mu\nu}$, that is a derived quantity[5] defined below.

In the nonuniform case, the six symmetrized distortions $e_{\mu\nu}(\vec{r})$ cannot vary arbitrarily, if lattice integrity is to be maintained (i.e. no defects such as dislocations). They are linked

by the St. Venant's 'compatibility' equations[9,10] of 1864 that ensure distorted unit cells fit together in a smoothly compatible way. With a double-Curl operation defining an Incompatibility or 'Inc' operation, in coordinate and Fourier space, the Cartesian-component constraints on $\mathbf{e}(\vec{r})$ are

$$Inc[\mathbf{e}(\vec{r})] \equiv \vec{\nabla} \times (\vec{\nabla} \times \mathbf{e}(\vec{r}))^T = 0; \ (2.3a)$$

$$Inc[\mathbf{e}(\vec{k})] \equiv \vec{k} \times \mathbf{e}(\vec{k}) \times \vec{k} = 0. \ (2.3b)$$

(Similar equations hold for $\mathbf{w}(\vec{r})$, but for the transitions considered here we take spontaneous local rotations to be zero.)

From (2.1), in the *displacement representation* where $\vec{u}(\vec{r})$ is the working variable, compatibility is satisfied as an identity since $Curl(Grad) \equiv 0$. Baus and Lovett[10] have proposed the distortion tensor $\mathbf{D}$ be taken as the working variable, with the St Venant compatibility equations then being field equation constraints to be satisfied, rather than identities. In an electromagnetic analogy[10] this is like working with the magnetic induction $\vec{B}$ rather than the vector potential $\vec{A}$, with $Div\vec{B} = 0$ then a Maxwell field equation to be satisfied, rather than a $Div(Curl) \equiv 0$ identity. The change to a distortion-tensor variable is natural and useful, since the free energy depends directly on the distortion; and the constrained minimization in the distortion reveals powerlaw anisotropic potentials[11–17], that are hidden in the more conventional displacement representation.

The elastic free energy is invariant under global uniform rotations[5]. Consider a line-element in the elastic medium, described by a small imbedded column-vector $\vec{a}$ at a site $\vec{r}$. Under distortion of the medium, it locally stretches or rotates to a vector $\vec{A}(\vec{r}) = [\mathbf{1} + \mathbf{D}(\vec{r})]\vec{a}$. Free energies F can depend only on the scalar product $\vec{A}(\vec{r})^T.\vec{A}(\vec{r}) = \vec{a}^T.[\mathbf{1} + \mathbf{D}]^T[\mathbf{1}+\mathbf{D}].\vec{a} \equiv \vec{a}^T.[\mathbf{1}+2\mathbf{E}].\vec{a}$, where $\vec{A}^T, \vec{a}^T$ are row vectors. The free energy $F(E_{\mu\nu})$ thus depends on components of the 'Lagrangian-strain' tensor[5] $E_{\mu\nu}$, that is a derived quantity, defined in terms of the basic distortion variable $D_{\mu\nu}$ by

$$\mathbf{E}(\vec{r}) \equiv \frac{1}{2}[\mathbf{D}^T + \mathbf{D}] + \frac{1}{2}\mathbf{D}^T\mathbf{D} = \mathbf{e}(\vec{r}) + \mathbf{g}(\vec{r}), \ (2.4)$$

where the 'geometric nonlinearity' is $\mathbf{g} \equiv \frac{1}{2}\mathbf{D}^T\mathbf{D}$.

It is convenient to consider $d(d+1)/2$ *physical* strains e_α that are linear combinations of the $d(d+1)/2$ Cartesian strains $e_{\mu\nu}$. For 2D lattices, with three Cartesian components, they are e_α with $\alpha = 1, 2, 3$: the compressional (e_1), deviatoric (e_2), and shear (e_3) strains. With X, Y transforming as 2D Cartesian coordinates, the physical strains transform as $e_1 \sim X^2 + Y^2, e_2 \sim X^2 - Y^2, e_3 \sim XY$, and are defined as[13]

$$e_1(\vec{r}) = \frac{c_1}{2}(e_{xx} + e_{yy}); e_2(\vec{r}) = \frac{c_2}{2}(e_{xx} - e_{yy});$$

$$e_3(\vec{r}) = \frac{c_3}{2}(e_{xy} + e_{yx}) = c_3 e_{xy}. \ (2.5a)$$

The physical Lagrangian-strains are similarly defined, so

$$E_1(\vec{r}) = \frac{c_1}{2}(E_{xx} + E_{yy}) = e_1 + g_1;$$

$$E_2(\vec{r}) = \frac{c_2}{2}(E_{xx} - E_{yy}) = e_2 + g_2;$$

$$E_3(\vec{r}) = c_3 E_{xy} = e_3 + g_3; \quad (2.5b)$$

where the physical geometric-nonlinearities are $g_1 = \frac{c_1}{2}(g_{xx} + g_{yy})$, $g_2 = \frac{c_2}{2}(g_{xx} - g_{yy})$, $g_3 = c_3 g_{xy}$. For square unit-cells in the high-temperature phase, the normalizing coefficients are chosen as $c_1 = \sqrt{2} = c_2$, and $c_3 = 1$, while for triangular unit cells $c_1 = c_2 = c_3 = 1$.

For 3D cubic lattices with six Cartesian strain components, the physical strains e_α with $\alpha = 1, 2, ..6$ are the compressional (e_1), deviatoric (e_2, e_3), and shear (e_4, e_5, e_6) symmetrized-distortions. These transform as one, two, and three dimensional irreducible representations of the cubic point group. For the cubic lattice, with X, Y, Z transforming as 3D Cartesian coordinates, the physical strains transform as $e_1 \sim X^2 + Y^2 + Z^2, e_2 \sim X^2 - Y^2, e_3 \sim X^2 + Y^2 - 2Z^2, e_4 \sim YZ, e_5 \sim ZX, e_6 \sim XY$, and are defined as[14,16]

$$e_1(\vec{r}) = \frac{1}{\sqrt{3}}(e_{xx} + e_{yy} + e_{zz});$$

$$e_2(\vec{r}) = \frac{1}{\sqrt{2}}(e_{xx} - e_{yy}); \ \ e_3(\vec{r}) = \frac{1}{\sqrt{6}}(e_{xx} + e_{yy} - 2e_{zz}) \ ;$$

$$e_4(\vec{r}) = 2e_{yz}, e_5(\vec{r}) = 2e_{zx}, e_6(\vec{r}) = 2e_{xy}. \quad (2.6a)$$

The physical Lagrangian-strains E_α are similarly defined so e.g. $E_1 = (E_{xx} + E_{yy} + E_{zz})/\sqrt{3} = e_1 + g_1$ where $g_1 \equiv (g_{xx} + g_{yy} + g_{zz})/\sqrt{3}$, and so on.

For the tetragonal lattice[16],

$$e_1(\vec{r}) = \frac{1}{\sqrt{2}}(e_{xx} + e_{yy});$$

$$e_2(\vec{r}) = \frac{1}{\sqrt{2}}(e_{xx} - e_{yy}); \ e_3(\vec{r}) = e_{zz}. \quad (2.6b)$$

and the physical shears are the same as (2.6a). These transform as irreducible representations of the tetragonal point group.

As noted in the Appendix, the St Venant constraint (2.3b) in Fourier space can be written in terms of the physical strains as

$$\sum_{\alpha=1,2...6} O_\alpha^{(s)} e_\alpha(\vec{k}) = 0, \ (2.7)$$

where $O_\alpha^{(s)}(\vec{k})$ are compatibility coefficients appropriate to the symmetry, labelled by shear components, $s = 3$ in 2D (one constraint), and $s = 4, 5, 6$ in 3D (three constraints). This is used in the Appendix to calculate the compatibility potentials.

The physical strains can be separated into N_{OP} order parameter strains labelled by $\alpha = \ell$ or $\{e_\ell\}$; and $n = [\frac{1}{2}d(d+1) - N_{OP}]$ non-OP strains, labelled by $\alpha = i$ or $\{e_i\}$. (An associated separation of the physical Lagrangian-strains for each transition into $\{E_\ell\}$ and $\{E_i\}$ is also made.) For a ferroelastic transition, the free energy $F = F_L + F_{non} + F_G$. The Landau part of the free energy $F_L(E_\ell)$ can be written as a sum of p-th order polynomial invariants in the OP Lagrangian-strains, that can be found by direct evaluation[11–15] for simple cases. The non-OP free energy $F_{non}(E_i)$ is taken as harmonic in the non-OP Lagrangian-strains. For simplicity we neglect symmetry-allowed anisotropic gradients[14,15], and consider only OP gradient-squared costs in the Ginzburg term $F_G(\vec{\nabla} E_\ell)$. For all 2D transitions, an exhaustive evaluation of the OP and OP-gradient invariants, and allowed OP/non-OP couplings, was carried out through the program ISOTROPY of Stokes and Hatch[15].

Then with a sum or integral ($\sum_{\vec{r}} \to \int d^d r/a_0$) over all positions $\vec{r}$ where a_0 is a lattice scale, the total variational free energy in terms of free energy densities f is

$$F = \sum_{\vec{r}} f_L(E_\ell) + f_G(\vec{\nabla} E_\ell) + f_{non}(E_i). \quad (2.8)$$

The Landau term f_L is not just an arbitrary Taylor series, but is a finite-sum expansion in terms of symmetry-allowed, invariant polynomials of physical OP Lagrangian-strains

$$f_L = C^{(2)}(T) I_2 + \sum_{p=3,\dots p_{max}} \sigma_p C^{(p)} I_p(E_\ell). \quad (2.9a)$$

The second order invariant $I_2 = \sum_\ell E_\ell^2$ is common to all transitions, and is separated out. The anharmonic elastic coefficients $C^{(p)} > 0$ are temperature-independent, and $\sigma_p = +1, -1$ are chosen signs, to get N_V minima. We consider an elastic coefficient $C^{(2)}(T) = (T - T_c){C_0}^{(2)}$ that would partially soften to zero on cooling to a temperature $T = T_c$, but is preempted by the first order transition. The Ginzburg and non-OP terms, with domain wall cost parameter b and $A^{(i)}$ elastic coefficients[26], are

$$f_G = \sum_\ell b(\vec{\nabla} E_\ell(\vec{r}))^2; \; f_{non} = \sum_i \frac{1}{2} A^{(i)} {E_i}^2(\vec{r}). \quad (2.9b)$$

The temperature-dependence of sound velocities[27] experimentally determine the linear slope ${C_0}^{(2)}$, and the extrapolated temperature T_c. The curvature of phonon spectrum at long wavelengths[27] determine b, that is related to domain-wall energy costs at short wavelengths. We take it to be positive $b > 0$; but for $b < 0$, one can add phenomenologically a symmetry allowed positive-coefficient, fourth-order gradient term, for stability.

B. General scaling and minimization procedure

We now follow a Barsch-Krumhansl procedure[18]: scaling all Cartesian distortions $D_{\mu\nu} \to \lambda D_{\mu\nu}$ or $e_{\mu\nu} \to \lambda e_{\mu\nu}, w_{\mu\nu} \to \lambda w_{\mu\nu}$ in a typical value λ; scaling all energy terms in E_0 ; and defining a transition temperature T_0. These three parameters are chosen in terms of the material-specific elastic constants, to make the Landau free energy simple. The parameters have physical meanings: since scaled terms are of order unity, the overall prefactor E_0 is the elastic energy per unit cell; the temperature $T_0 (> T_c)$ is the first-order transition temperature that pre-empts the second-order elastic-constant softening at T_c; and λ is the spontaneous-strain magnitude at T_0, since the scaled strain is chosen to be unity at transition.

Since the physical distortions are linear combinations of the Cartesian distortions, they change as $e_\alpha \to \lambda e_\alpha$, and the physical Lagrangian-strains change as

$$E_\alpha \to \lambda E_\alpha(\lambda) \equiv \lambda(e_\alpha + \lambda g_\alpha). \quad (2.10)$$

Henceforth e_α is the *scaled* symmetrized-distortion or scaled strain. The (scaled) geometric nonlinearity g_α carries a prefactor λ. The free energy changes as

$$F(E_\alpha) \to F[\lambda E_\alpha(\lambda)] \equiv E_0 \bar{F}[E_\alpha(\lambda)], \quad (2.11a)$$

defining a dimensionless $\bar{F}[E_\alpha(\lambda)] = \sum_{\vec{r}} \bar{f}[E_\alpha(\lambda)]$ where the scaled dimensionless free-energy densities are

$$\bar{f}[E_\alpha(\lambda)] \equiv \bar{f}_L[E_\ell(\lambda)] + \bar{f}_G[\vec{\nabla} E_\ell(\lambda)] + \bar{f}_{non}[E_i(\lambda)]. \quad (2.11b)$$

These terms contain dimensionless scaled coefficients that absorb the 'external' λ powers of (2.10) as

$$C_p \equiv C^{(p)} \lambda^p / E_0; \; A_i \equiv A^{(i)} \lambda^2 / E_0; \; \xi^2 \equiv b\lambda^2 / {a_0}^2 E_0. \quad (2.12)$$

Here a dimensionless length ξ has a lattice constant a_0 scale, from a substitution as below in the Ginzburg term $\vec{\nabla} \to \vec{\Delta}/a_0$, where $\vec{\Delta}$ is a discrete-difference operator on a computational grid.

A scaled temperature[18] τ absorbs the harmonic-term material dependence, and is defined as

$$\tau(T) = (T - T_c){C_0}^{(2)} \lambda^2 / E_0 \equiv (T - T_c)/(T_0 - T_c), \quad (2.13)$$

where the transition temperature $T_0 > T_c$ is determined by requiring $\tau(T_0) = (T_0 - T_c){C_0}^{(2)} \lambda^2 / E_0 = 1$ or

$$T_0 = T_c + E_0/({C_0}^{(2)} \lambda^2). \quad (2.14)$$

At the first-order Landau transition temperature at a universal value $\tau(T_0) = 1$, the nontrivial or 'martensite' wells are degenerate with the trivial or 'austenite' well; while T_c is the lower spinodal, where at a universal value $\tau(T_c) = 0$, the metastable austenite well disappears. The upper spinodal T_{up}

where the martensite-variant wells disappear, turns out also to have a universal value $\tau(T_{up}) = \tau_{up}$ for three of the four 3D transitions.

A constrained minimization of the scaled free energy $\bar{f}[E_\alpha(\lambda)]$ of (2.11b) with respect to e_α, would, for general λ, fix the parameters λ, E_0, and yield an effective OP-OP interaction potential. However because of geometric nonlinearities the calculation is involved, and we perturbatively evaluate the scaling parameters and compatibility potentials, as below. Corrections can in principle, be calculated.

We make a simplifying assumption that the typical spontaneous distortion is small compared to unity

$$\lambda \ll 1, \qquad (2.15)$$

and for most materials this is indeed a few per cent, $\lambda \sim 10^{-2}$. Then the scaled physical Lagrangian-strains $E_\alpha(\lambda) = e_\alpha + \lambda g_\alpha$ are approximated by the scaled physical symmetrized-distortions,

$$E_\ell(\lambda) \simeq E_\ell(0) = e_\ell; E_i(\lambda) \simeq E_i(0) = e_i. \ (2.16)$$

In fact, this approximation of dropping geometric nonlinearities in the Lagrangian-strains is commonly made without specific comment. In the conventional (unscaled) displacement representation it is implicitly justified as a long-wavelength truncation: in Fourier space the strain tensor is $\sim [\vec{q}\vec{u}(q)]_{\mu\nu}$, while the geometric nonlinearity is $g_{\mu\nu}(\vec{q}) \sim [\vec{q}\vec{u}(\vec{q})]^2{}_{\mu\nu}$, that is higher order in $\vec{q} \to 0$. Instead, in the (scaled) strain representation, the neglect of geometric nonlinearities is seen as the leading term in a small-parameter expansion in λ, that could be systematically corrected.

The scaled free energy densities of (2.11b) then become $\bar{f}[E_\alpha(\lambda)] \simeq \bar{f}(e_\alpha)$, to leading order in λ, separately for each distinct symmetry-invariant term,

$$\bar{f}(e_\alpha) = \bar{f}_L(e_\ell) + \bar{f}_G(\vec{\Delta}e_\ell) + \bar{f}_{non}(e_i), (2.17)$$

From (2.9a), (2.9b), (2.12) and (2.13),

$$\bar{f}_L(e_\ell) = (\tau - 1)\sum_\ell {e_\ell}^2 + f_0(e_\ell), \quad (2.18a)$$

$$f_0(e_\ell) \equiv \sum_\ell {e_\ell}^2 + \sum_p \sigma_p C_p I_p(e_\ell), \quad (2.18b)$$

$$\bar{f}_G(\vec{\nabla}e_\ell) = \sum_\ell \xi^2(\vec{\Delta}e_\ell)^2, \ \ \bar{f}_{non}(e_i) = \sum_i \frac{A_i}{2}{e_i}^2. \ (2.18c)$$

Here as mentioned previously, $\vec{\Delta} = (\Delta_x, \Delta_y, \Delta_z)$ has discrete forward-difference operator components on a cubic computational grid.

We pause to relate the unscaled harmonic coefficients $A^{(i)}$ of (2.9) to the material elastic constants. The elastic energy is[26] $E = \frac{1}{2}\sum_{\alpha,\beta} C_{\alpha\beta}x_\alpha x_\beta$ where with $\alpha = 1, 2, ..6$, the $\{x_\alpha\}$ are Cartesian strains written as a column vector such as $x_1 = e_{xx}, x_4 = 2e_{yz}$. In the cubic case, there are three independent elastic constants in the Voigt notation, $C_{11}, C_{12}, C_{44}(= C_{55} = C_{66})$. Writing Cartesian in terms of physical strains, through (2.6a) and (A9), the energy E is diagonalized, and a comparison with (2.9) yields $C_{11} - C_{12} = C^{(2)}(T), C_{11} + 2C_{12} = A^{(1)}, C_{44} = A^{(4)}$. It is useful to introduce the elastic anisotropy parameter[26] $A(T) \equiv 2C_{44}/(C_{11} - C_{12})$, where $A > 1$ (or $A < 1$) corresponds to greater stiffness in the body diagonal $< 111 >$ directions (or cubic axis $< 100 >$ directions). Strongly anisotropic materials can have $A \sim 10$. Then from (2.12), the scaled shear coefficient $A_4(= A_5 = A_6)$, and the scaled compression coefficient A_1 are both in terms of the elastic anisotropy parameter $A(T = T_0)$ at transition,

$$A_4 = A(T_0); \ A_1 = \gamma A(T_0); \ \gamma \equiv [(C_{11}+2C_{12})/C_{44}]. \ (2.18d)$$

The elastic constant ratio $\gamma = A_1/A_4(= A_1/A_5 = A_1/A_6)$, that enters the compatibility potentials, can for simplicity be set in simulations to a constant, say $A^{(1)}/2A^{(4)} \sim 1$ as in[11] FePd. [For xy plane distortions, the shear term is $(A_6/2)4{e_{xy}}^2$, so from (2.5a) the scaled 2D shear coefficient appearing later is also proportional to the anisotropy at transition.] Finally we note that from (2.12), the scaled Ginzburg coefficient is similarly $\xi^2 \sim (b/a_0^2)A(T_0)$.

We now return to the main argument. A constrained minimization of the harmonic non-OP terms in (2.18c) as in the Appendix yields the non-OP in terms of the OP strains, $e_i(\vec{k}) = \sum_\ell B_{i\ell}(\vec{k})e_\ell(\vec{k})$ where the $B_{i\ell}$ coefficients are in terms of the coefficients ${O_\alpha}^{(s)}$ of (2.7). Substituting back in the harmonic term, $\bar{F}_{non}[e_i(e_\ell)] \equiv \bar{F}_{compat}(e_\ell)$ induces the St Venant term

$$\bar{F}_{compat}(e_\ell) = \frac{1}{2}A_1 \sum_{\vec{k},\ell,\ell'} U_{\ell\ell'}(\vec{k})e_\ell(\vec{k})e^*_{\ell'}(\vec{k}). \ (2.19)$$

The compatibility kernel $A_1 U_{\ell\ell'}(\vec{k}) \equiv \sum_i A_i B_{i\ell}(\vec{k})B^*_{i\ell'}(\vec{k})$ is evaluated for each transition in the Appendix, and is essentially dependent only on the wave-vector direction $\hat{k}$, independent of the magnitude $|\vec{k}|$. In coordinate space, the compatibility potential is hence an anisotropic powerlaw with a falloff exponent equal to the dimensionality[11–17,23] $U_{\ell\ell'}(\vec{R}) \sim 1/R^d$. (Write the Fourier integral of $U_{\ell\ell'}(\hat{k})$and change the wave-vector integration variable $|\vec{k}| \to |\vec{k}|/R$: the exponent simply comes from the phase space dimension.)

We focus on the Landau term $\bar{f}_L$. To find the minima in OP space it is convenient to work in polar coordinates, following Toledano and Toledano[6]. For example the $N_{OP} = 2$ dimensional 'vector' in OP space is $\vec{e} = (\varepsilon\cos\phi, \varepsilon\sin\phi)$, where the 'radial' variable is

$$\varepsilon \equiv |\vec{e}| = [\sum_\ell {e_\ell}^2]^{1/2}, \ (2.20)$$

and the Landau free energy density is

$$\bar{f_L}(\vec{e}) = \bar{f_L}(\varepsilon,\phi) = (\tau-1)\varepsilon^2 + f_0(\varepsilon,\phi), \ (2.21)$$

where the transition-specific f_0 is temperature independent. We demand that the nontrivial Landau minima are at $m = 1, 2, ..N_V$ equivalent points $\{\varepsilon_m, \phi_m\}$, with the same radii $\varepsilon_m = \bar{\varepsilon}$ in OP space. The conditions are:

$$\frac{\partial \bar{f_L}(\varepsilon_m,\phi_m)}{\partial \varepsilon_m} = 2(\tau-1)\varepsilon_m + \frac{\partial f_0(\varepsilon_m,\phi_m)}{\partial \varepsilon_m} = 0, \ \ (2.22a)$$

locating the martensitic minima in the radial direction at a temperature-dependent $\varepsilon = \varepsilon_m = \bar{\varepsilon}(\tau)$; and

$$\frac{\partial \bar{f_L}(\varepsilon_m,\phi_m)}{\partial \phi_m} = \frac{\partial f_0(\varepsilon_m,\phi_m)}{\partial \phi_m} = 0, \ \ (2.22b)$$

locating the minima in the azimuthal direction at a temperature-independent $\phi = \phi_m$. At transition $\tau = 1$, we also demand that the nonzero minima on a N_{OP}-dimensional 'sphere' of radius $\bar{\varepsilon}(\tau = 1) = 1$, become degenerate with the trivial minimum $\bar{f_L}(\vec{e} = 0) = 0$. Hence

$$f_0(\varepsilon_m = 1, \phi_m) = 0. \ (2.22c)$$

Above an upper spinodal $\tau = \tau_{up}$ the radial solutions $\bar{\varepsilon}(\tau)$ become imaginary, and there is only the trivial austenite minimum. It is convenient for later use to define the Landau free energy at minima

$$\bar{f_L}(\tau) \equiv \bar{f_L}(\bar{\varepsilon},\phi_m) \equiv \bar{\varepsilon}(\tau)^2 g_L(\tau), \ (2.22d)$$

where $g_L(\tau)$ changes sign at the Landau transition.

With τ defined, we choose the remaining two scaling parameters λ, E_0 so the f_0 conditions of (2.22b), (2.22c) are satisfied. It is useful from (2.21) to separate the angular dependence into a part $\Delta f_0(\varepsilon,\phi) \equiv f_0(\varepsilon,\phi) - f_0(\varepsilon,\phi_m)$ that vanishes in the minimum angular directions, so

$$\bar{f_L}(\varepsilon,\phi) \equiv [(\tau-1)\varepsilon^2 + f_0(\varepsilon,\phi_m)] + \Delta f_0(\varepsilon,\phi), \ (2.23a)$$

and $\bar{\varepsilon}(\tau)$ is determined through minimization of only

$$\bar{f_L}(\varepsilon,\phi_m) = [(\tau-1)\varepsilon^2 + f_0(\varepsilon,\phi_m)]. \ (2.23b)$$

There is always an overall material constant E_0 for the Landau energy $f_L = E_0 \bar{f_L}$, that absorbs unknown higher-order elastic coefficients, and can be treated as a fitting parameter. Since we work only to leading order in λ, any material-independence found in the scaled $\bar{f_L}(\vec{e})$ contributions is strictly speaking only *quasi*-universal. Landau quasi-universality can be of three kinds: (i) *strong*, i.e. the scaled $\bar{f_L}(\varepsilon,\phi)$ is independent of material parameters for all ε, ϕ; (ii) *medium*, i.e. material coefficients appear only in Δf_0 that vanishes at $\phi = \phi_m$, so along minima angles, $\bar{f_L}(\varepsilon,\phi_m)$ is material-independent; and finally (iii) *weak*, with residual material-dependence in $\bar{f_L}(\varepsilon,\phi_m)$, and hence in the OP magnitude $\bar{\varepsilon}(\tau)$ (that is however still unity at transition for all materials). The tetragonal/orthorhombic and cubic/ tetragonal; the cubic/trigonal ; and the cubic/orthorhombic transitions (with unscaled material coefficients of respectively $N_{mat} = 3, 3, 4$ and 6), turn out to have quasi-universality in $\bar{f_L}$ of respectively the first, second and third kinds. Table I summarizes the generic numbers for all transitions considered, with different materials with the same transition falling into the same 'quasi-universality class'.

Going back to unscaled variables denoted by primes, the unscaled entropy-density difference relative to the austenite from the Landau term is $s_L{}'(T) = -\partial f_L'(\bar{\varepsilon}'(\tau),\phi_m)/\partial T$. Since the derivative of (2.22a) with respect to $\bar{\varepsilon}'(\tau)$ vanishes, only the explicit τ-dependence of $\bar{f_L}$ contributes. The scaled entropy-density difference is

$$\bar{s}_L(\tau) \equiv [(T_0 - T_c)/E_0] s_L{}'(\tau) = -\bar{\varepsilon}(\tau)^2, \ (2.24)$$

and is (minus) unity at transition. Of course there are other free energy terms, and hysteresis from domain-wall textures, so this is just a formal result.We will consider *proper* ferroelastic transitions with free energy nonlinearities in the OP strain driving the transition (without intracell shuffles); with high/low temperature unit-cell symmetries having a group/subgroup relationship; and without coupling to other fields. (There are also improper ferroelastics, with only harmonic terms in strains, that are however coupled to other fields such as electric polarization or magnetization, whose nonlinearities can induce a structural transition[3].)

In Secs. III–V we consider scaling of the Landau free energy (and other terms), for four 3D transitions with $N_{OP} = 1, 2, 3$ and for five 2D transitions with $N_{OP} = 1, 2$, presented in increasing number of variants $N_V = 2, 3, 4, 6$. Some cases had been scaled earlier[12,13,18] but are summarized here for completeness. The final results for the minima are summarized in Table I.

III. TRANSITIONS WITH $N_V = 2$

We consider one 3D transition and two 2D transitions, all with $N_V = 2$ low temperature variants and a single order parameter (OP) component $N_{OP} = 1$, with the number of non-OP variables $n = \frac{1}{2}d(d+1) - N_{OP}$. The transitions are: (a) tetragonal/orthorhombic in 3D ($n = 5$); and (b) square/rectangle (that includes square/ rhombus); and (c) rectangle-oblique cases (all $n = 2$). See Figs 1 and 2.

A. Tetragonal/orthorhombic case in 3D: $N_V = 2, N_{OP} = 1, n = 5$

There are two deviatoric distortions e_2, e_3 in 3D, and the single ($N_{OP} = 1$) order parameter is $e_2 \sim X^2 - Y^2$ that can change a tetragonal square-cross-section to an orthorhombic rectangular-cross-section. Since there are two possible such

rectangular elongations (along mutually perpendicular directions), one expects two possible variants, as in Fig 2. The tetragonal point group G =$P4/mmm$ with $\nu_G = 16$ elements goes in a symmetry-lowering transition, to the orthorhombic subgroup g =$Pmmm$ with $\nu_g = 8$ elements[6]. The orthorhombic group describes symmetries of a unit cell with a particular rectangular orientation, corresponding to one variant. The ratio of the number of elements in a point group to that in a subgroup, or dimension of the coset G/g, is an integer, that we assume[6] corresponds to the number of variants. Thus here there are $N_V = \nu_G/\nu_g = 16/8 = 2$ variants, as expected. The ratio of the number of (rotational) elements in the point group elements, has been taken to be the number of variants[2], yielding the same result $8/4 = 2$ here, and in other cases. (See however, Section VI below.)

For these two variants in a first order transition, we need up to $p_{max} = 6$ even-order strain invariants I_p. The unscaled free energy, with sign choices $\sigma_4 = -1, \sigma_6 = +1$ is $f_L = C^{(2)}I_2 - C^{(4)}I_4 + C^{(6)}I_6$, where $I_p = {e_2}^p$ are invariants, so there are $N_{mat} = 3$ material constants. With $e_2 \to \lambda e_2$ and $C_p \equiv \lambda^p C^{(p)}/E_0$ as in (2.12), the scaled Landau free energy density $\bar{f}_L = f_L/E_0$ is as in (2.21):

$$\bar{f}_L(e_2) = (\tau - 1)e_2^2 + f_0(e_2), \qquad (3.1)$$

where the temperature-independent f_0 is

$$\bar{f}_0(e_2) = e_2^2 - C_4 e_2^4 + C_6 e_2^6. \quad (3.2)$$

The conditions (2.22a), (2.22c) for degenerate minima are $\partial f_0/\partial\varepsilon + 2(\tau - 1)\varepsilon = 0$, and $f_0(1) = 0$. This fixes the two coefficients

$$C_4 = 2;\ C_6 = 1, \qquad (3.3)$$

achieved by choosing the two scaling parameters as

$$\lambda = (C^{(4)}/2C^{(6)})^{1/2}; \quad E_0 = C^{(6)}(C^{(4)}/2C^{(6)})^3. \quad (3.4)$$

Then f_0 becomes a perfect square, and

$$\bar{f}_L(e_2) = (\tau - 1)e_2^2 + e_2^2(e_2^2 - 1)^2, \qquad (3.5)$$

manifestly showing the triple-minima degeneracy at $f_L = 0$ for $\tau = 1$. The variant minima are at $\pm\bar{\varepsilon}(\tau)$ where the order parameter magnitude

$$\bar{\varepsilon}(\tau) = \left\{\frac{2}{3}[1 + \sqrt{1 - 3\tau/4}]\right\}^{1/2}, \qquad (3.6)$$

is unity at transition. Here from (2.22d) the variable used later in pseudospin hamiltonians is $\bar{f}_L/\bar{\varepsilon}^2 \equiv g_L = \tau - 1 + (\bar{\varepsilon}^2 - 1)^2$. Barriers at $\bar{\varepsilon}_b(\tau) = \left\{\frac{2}{3}[1 - \sqrt{1 - 3\tau/4}]\right\}^{1/2}$ exist in the range $0 < \tau < \tau_{up} = 4/3$. The barriers merge with the metastable martensite (or metastable austenite) minimum at the upper spinodal $\tau = 4/3$ (or lower spinodal $\tau = 0$).

Since $\bar{f}_L[\bar{\varepsilon}(\tau)]$ is independent of material parameters, this is quasi-universality of the first kind, with $f_L = E_0\bar{f}_L$ having only an overall material dependence through E_0, that absorbs the higher-order elastic constants.

With the OP sign formally written as an angle, $e_2 = |\varepsilon|\cos\phi$ where $|e_2| = |\varepsilon|$, and the minima are at $\phi_m = 2(m-1)\pi/N_V$, with $m = 1, 2(= N_V)$, where $\sin 2\phi_m = 0$. At transition, the nontrivial Landau minima fall at $N_V = 2$ points at ± 1 on a line in the $N_{OP} = 1$ dimensional order parameter space, as in Fig 3 and Table I. The number of distinct martensite/martensite domain walls between variant pairs is $N_W = 1$.

Had we included an eighth order invariant $\sim C^{(8)}{e_2}^8$ in (3.2), the minimum condition would become $\tau - 2\varepsilon^2 + 3\varepsilon^4 + 4C_8\varepsilon^6 = 0$. Here the new scaled coefficient is $C_8 = C^{(8)}\lambda^8/E_0 = (C^{(8)}/C^{(6)})\lambda^2$. Assuming the ratio of eighth and sixth order unscaled constants is not too large, the shift in the roots arising from $C_8 \sim \lambda^2 \ll 1$ is negligible. The extra eighth order invariant is thus 'irrelevant', in the sense that the polyhedral minima remain essentially unchanged, justifying the finite-sum restriction to $p_{max} = 6$ of the polynomial expansion.

The scaled Ginzburg term is $\bar{f}_G = \xi^2(\vec{\Delta}e_2)^2$. There are $n = 5$ non-OP strains, namely the compression $e_1 \sim X^2 + Y^2$; the other deviatoric strain $e_3 \sim X^2 + Y^2 - 2Z^2$; and the three shears e_4, e_5, e_6. Using the three compatibility constraints of (2.7) to eliminate the shears, and minimizing in e_1, the non-OP strains are determined by the OP. Substituting into the harmonic non-OP terms yields an OP compatibility potential term as in (2.19): $\bar{f}_{non}(e_i) = \sum_{i=1,3,4,5,6}(A_i/2){e_i}^2 \to \bar{f}_{compat}(e_2)$ where

$$\bar{f}_{compat} = \frac{A_1}{2}U(\vec{k})|e_2(\vec{k})|^2, \qquad (3.7)$$

and the kernel $U(\vec{k})$ is given in (A26) of the Appendix.

B. Square/rectangle case: $N_V = 2, N_{OP} = 1, n = 2$

The single 2D deviatoric distortion $e_2 \sim X^2 - Y^2$ turns a square to a rectangle. Since the rectangular elongation can be along two axes, one expects two variants, as in Fig 1. The point group G = $p4mm$ for a square unit cell has $\nu_G = 4$ elements, while the subgroup g for the rectangle is $p2mm$ with $\nu_g = 2$ elements. Thus the number of variants is[15] $N_V = \nu_G/\nu_g = 2$ as expected, and we again need up to $p_{max} = 6$ order invariants. The scaled Landau free energy $\bar{f}_L(e_2)$ is the same form as (3.5) above, so the minima are at the same $\pm\bar{\varepsilon}(\tau)$ of (3.6).

The scaled Ginzburg term is $\bar{f}_G = \xi^2(\vec{\Delta}e_2)^2$. There are $n = 2$ non-OP strains $e_1 \sim X^2 + Y^2, e_3 \sim XY$, and the harmonic free energy term is $\bar{f}_{non}(e_i) = \frac{1}{2}\sum_{i=1,3} A_i|e_i(\vec{k})|^2$. This induces a compatibility kernel[11–13,15] $U(\vec{k})$ as in (A4) of the Appendix.

The square/rhombus transition has $N_V = 2, N_{OP} = 1, n = 2$, and the 2D shear physical distortion $e_3 \sim XY$ as the single order parameter. However this is not an independent transition[15], since e_2 and e_3 interconvert through a global rotation of Cartesian axes by $\pi/4$. Nonetheless, as an exercise the symmetry group of the square is G = $p4mm$ with $\nu_G = 4$ components, while the rhombus symmetry is g = P2 with $\nu_g = 2$ elements, so $N_V = 2$. The scaled Landau free energy is $\bar{f}_L(e_3)$, formally as in (3.5),

$$\bar{f}_L(e_3) = (\tau - 1)e_3^2 + e_3^2(e_3^2 - 1)^2, (3.8)$$

with two nonzero minima at the same values $e_3 = \pm\bar{\varepsilon}(\tau)$.

The Ginzburg term is $\bar{f}_G = \xi^2(\vec{\Delta}e_3)^2$. The $n = 2$ non-OP strains are now compressional and deviatoric, $e_1 \sim X^2 + Y^2$ and $e_2 \sim X^2 - Y^2$, with the harmonic[11–13] $\bar{f}_{non} = \frac{1}{2}\sum_{i=1,2} A_i|e_i|^2$ inducing a kernel $U(\vec{k})$ as in (A5) of the Appendix.

There is another symmetry-allowed transition[13,15], namely the square/centered rectangle. In addition to strain, as in the square/rectangle, it also involves a shuffle because of the center site, so is not considered here.

C. Rectangle/oblique case: $N_V = 2, N_{OP} = 1, n = 2$

The shear physical distortion e_3 changes a rectangle to an oblique polygon, and is the single $N_{OP} = 1$ order parameter. The point group G =$p2mm$ with $\nu_G = 2$ elements goes to the subgroup g= $p2$ with $\nu_g = 1$ elements, so there are $N_V = 2$ variants. The $\bar{f}_L(e_3)$ Landau part is the same as the square/rhombus case of (3.8); however the $n = 2$ non-OP contributions are harmonic in the combinations $e_\pm = (e_1 \pm e_2)/2$, as $\bar{f}_{non} = \frac{A_+}{2}{e_+}^2 + \frac{A_-}{2}{e_-}^2$. This yields a different compatibility kernel[13,15]in $\bar{f}_{compat} = \frac{A_1}{2}U(\vec{k})|e_3(k)|^2$, as in (A6).

IV. TRANSITIONS WITH $N_V = 3$

We consider two transitions with $N_V = 3$ variants, and $N_{OP} = 2$ order parameter (OP) components, but with different numbers n of non-OP strains. They are the (a) cubic/tetragonal transition in 3D ($n = 4$); and (b) triangle/centered rectangle in 2D ($n = 1$). See Figs 1 and 2.

A. 3D cubic/tetragonal case: $N_V = 3, N_{OP} = 2, n = 4$

There are three axes along which the cubic unit cell can elongate, to make a tetragonal cell, so one expects three variants, as in Fig 2.The cubic symmetry group G = $Pm\bar{3}m$ with $\nu_G = 48$ elements goes to the tetragonal group g = $P4/mmm$ with $\nu_g = 16$ elements, so there are[6] $N_V = 3$ variants, as expected. The variants are generated by joint action of the $N_{OP} = 2$ order parameters that are the two 3D deviatoric strains[13,18,28], with the vector in OP space chosen as $\vec{e} = (e_3, e_2) \sim (\frac{1}{\sqrt{6}}\{X^2 + Y^2 - 2Z^2\}, \frac{1}{\sqrt{2}}\{X^2 - Y^2\})$.

The cubic/tetragonal Landau free energy has been considered by Barsch and Krumhansl and others[18,28]. The invariants $\{I_p\}$ under the cubic point group, up to a maximum order $p_{max} = 4$, are $I_2 = e_3^2 + e_2^2 \equiv \varepsilon^2$, $I_4 = I_2^2$, and a third-order invariant $I_3 = e_3^3 - 3e_2^2e_3$. This is explicitly seen to be a scalar under cubic-symmetries, as it can be written with (2.6a) in terms of invariants $(XYZ)^2$ and $X^q + Y^q + Z^q$ with $q = 2, 4, 6$. From BK scalings as before, and sign choices $\sigma_3 = -1, \sigma_4 = +1$ for three minima, we have $\bar{f}_L = (\tau - 1)\vec{e}^2 + f_0(e_3, e_2)$, where the temperature-independent f_0 of (2.18a) is

$$f_0 = I_2 - C_3I_3 + C_4I_4, (4.1)$$

and the unscaled elastic constants $C^{(3)}$, $C^{(4)}$ are related to the scaled ones as

$$C_3 = C^{(3)}\lambda^3/E_0; \quad C_4 = C^{(4)}\lambda^4/E_0. \quad (4.2)$$

In polar coordinates in OP space[6], with $\vec{e} \equiv (e_3, e_2) = \varepsilon(\cos\phi, \sin\phi)$ of magnitude

$$\varepsilon \equiv |\vec{e}| = [{e_3}^2 + {e_2}^2]^{1/2}, \quad (4.3)$$

the symmetry in OP space is manifestly carried by the third-order invariant,

$$I_3 = \varepsilon^3(\cos^3\phi - 3\cos\phi\sin^2\phi) = \varepsilon^3\cos 3\phi. \quad (4.4)$$

Then f_0 in the form of (2.23), with $\eta_3 \equiv \cos 3\phi$ is

$$f_0 = \varepsilon^2 - C_3\varepsilon^3 + C_4\varepsilon^4 + \Delta f_0; \quad (4.5a)$$

$$\Delta f_0 = C_3\varepsilon^3(1 - \eta_3). \quad (4.5b)$$

The angular dependence is in $\Delta f_0 \sim -\cos 3\phi$. The radial minima and degeneracy conditions on f_0 with $\eta_3(\phi_m) = 1$, yield $2 - 3C_3 + 4C_4 = 0$ and $1 - C_3 + C_4 = 0$, fixing the two coefficients as

$$C_3 = 2; \quad C_4 = 1, \quad (4.6)$$

achieved by choosing scaling parameters

$$\lambda = C^{(3)}/2C^{(4)}; \; E_0 = C^{(4)}(C^{(3)}/2C^{(4)})^4. \quad (4.7)$$

Then $\bar{f}_L(e_3, e_2)$ and hence $\bar{\varepsilon}(\tau)$ is independent of material constants, i.e. there is quasi-universality of the first kind. The $N_V = 3$ variant minima of $f_0(\varepsilon, \phi)$ are at angles $\eta_3(\phi_m) = \cos 3\phi_m = 1$, and radius $\varepsilon_m = \bar{\varepsilon}(\tau)$, where

$$\sin 3\phi_m = 0;\ \phi_m = \frac{2(m-1)\pi}{N_V},\ m = 1,2,3(=N_V);\ (4.8)$$

$$\bar{\varepsilon}(\tau) = \frac{3}{4}[1+\sqrt{1-8\tau/9}].\ (4.9)$$

For $\tau = 1$, $\bar{\varepsilon}(\tau) = 1$, as required, and the upper spinodal is universal, $\tau = \tau_{up} = 9/8$. The saddle-point barriers are at radius $\bar{\varepsilon}_b(\tau) = \frac{3}{4}[1-\sqrt{1-8\tau/9}]$, and angles $\phi_{bm} = (2m-1)\pi/3$.

At transition the minima of the Landau free energy fall on the $N_V + 1 = 4$ vertices and center of a rightward-pointing equilateral triangle[13,28] inscribed in a unit circle in $N_{OP} = 2$ dimensional OP space, with corners at $(e_3, e_2) = (1,0), (-1/2, \pm\sqrt{3}/2)$. (For a different sign choice $\sigma_3 = +1$, the triangle merely changes direction.) See Fig 3 and Table I. The upper bound on the possible types of domain wall between pairs of variants is $N_W = N_V!/[2!(N_V-1)!] = N_V(N_V-1)/2 = 3$.

The scaled Landau free energy $\bar{f}_L = (\tau-1)\varepsilon^2 + f_0$ in OP components with the choice (4.6) is

$$f_0 = I_2 - 2I_3 + I_4 = e_3^2 + e_2^2 - 2(e_3^3 - 3e_3e_2^2) + (e_3^2+e_2^2)^2$$

$$= (1+2e_3)(3e_2^2 - e_3^2 + 2e_3 - 1) + (\bar{e}^2-1)^2,\ (4.10a)$$

where the second equation[13] explicitly shows the fourfold degenerate roots of $f_L = 0$ at transition.

In polar coordinates as in (2.23),

$$\bar{f}_L(\varepsilon,\phi) = [(\tau-1)\varepsilon^2 + \varepsilon^2(\varepsilon-1)^2] + \Delta f_0,\ \ (4.10b)$$

where $\Delta f_0 \equiv f_0(\varepsilon,\phi) - f_0(\varepsilon,\phi_m) = 2(1-\eta_3)\varepsilon^3$ vanishes in the angular directions $\phi = \phi_m$ of the minima. As $\bar{f}_L(\bar{\varepsilon},\phi)$ is material-independent, there is again quasi-universality of the first kind. Here from the definition of (2.22d), $g_L = \tau - 1 + (\bar{\varepsilon}-1)^2$.

The Ginzburg term is $\bar{f}_G = \xi^2[(\vec{\Delta}e_3)^2 + (\vec{\Delta}e_2)^2]$. There are $n = 4$ non-OP compressional e_1, and shear strains e_4, e_5, e_6, that can be written in terms of the OP strains, so $e_i = \sum_{\ell=2,3} B_{i\ell}e_\ell$ with $i = 1,4,5,6$. Substituting into the non-OP harmonic terms yields the cubic/ tetragonal potential with the 2×2 matrix kernel of (2.19), given in (A23) of the Appendix. The 3D relaxational OP strain simulations[14] did not explicitly state the kernel, now given here for completeness.

B. Triangle/centred-rectangle case: $N_V = 3, N_{OP} = 2, n = 1$

There are three ways to convert an equilateral to an isosceles triangle, with the unit cell of the (equilateral) triangle changing to a centered rectangle, so one expects three variants, as in Fig 1. The OP are 2D $N_{OP} = 2$ deviatoric and shear strains, with the OP vector chosen as $\vec{e} = (e_2, e_3) \sim \frac{1}{2}(X^2 - Y^2, XY)$. The triangle point group G= $p6mm$ with $\nu_G = 6$ elements goes to the centred rectangle subgroup g = $c2mm$ with $\nu_g = 2$ elements, so there are[15] $N_V = 3$ variants, as expected. The third-order invariant under $\pi/3$ rotations of the triangular lattice is now $I_3 = e_2^3 - 3e_2e_3^2$. For $(X,Y) = R(\cos\alpha, \sin\alpha)$, one finds $I_3 = (R^3/8)\cos 6\alpha$, manifestly invariant under the $\alpha \to \alpha + \pi/3$ triangular symmetry. The scaling parameter choices are as before. The final scaled Landau free energy[13] is formally similar to the cubic/tetragonal case of (4.10a), with e_2 and e_3 interchanged,

$$f_0 = I_2 - 2I_3 + I_4 = e_2^2 + e_3^2 - 2(e_2^3 - 3e_2e_3^2) + (e_2^2+e_3^2)^2.\ (4.11)$$

At transition the $N_V + 1 = 4$ degenerate Landau minima again fall on the three vertices and at the center of an equilateral triangle inscribed in a unit circle. The maximum number of domain wall types is $N_W = 3$.

The Ginzburg terms are the same as above, while the compatibility potential in 2D, is of course different. The single $n = 1$ non-OP (compressional) strain is $e_1 = -\sum_{\ell=2,3} O_\ell e_\ell / O_1$ from the 2D compatibility constraint. Substitution into the harmonic term as in (2.19) immediately yields[13,15], $\bar{f}_{non} = (A_1/2)|e_1(\vec{k})|^2 \to \bar{f}_{compat}(e_2, e_3)$ with a 2×2 compatibility-kernel matrix of (A2).

V. TRANSITIONS WITH $N_V = 4$

We consider two transitions with $N_V = 4$ variants, and different order parameter (OP) components. They are the (a) cubic/trigonal case in $3D$ ($N_{OP} = 3$, $n = 3$); and (b) square/oblique case in $2D$ ($N_{OP} = 2$, $n = 1$). See Figs 1 and 2.

A. Cubic/trigonal case: $N_V = 4, N_{OP} = 3, n = 3$

The distortion acts along body diagonals of the cube and the $N_{OP} = 3$ shears are the three components of the OP vector $\vec{e} = (e_4, e_5, e_6) \sim (YZ, ZX, XY)$. With the cubic group G = $Pm\bar{3}m$ with $\nu_G = 48$ going to the trigonal or rhombohedral subgroup g = $P\bar{3}1m$ with $\nu_g = 12$, there are[6] $N_V = 4$ shear-induced variants. The four invariants up to order $p_{max} = 4$ are $I_2 = e_4^2 + e_5^2 + e_6^2$; $I_3 = e_4e_5e_6$; $I_4 = e_4^4 + e_5^4 + e_6^4$; and $I_4' = {I_2}^2$, with $N_{mat} = 4$ material coefficients. The scaled Landau free energy is

$$\bar{f}_L = (\tau-1)I_2 + f_0(e_4, e_5, e_6),\quad (5.1a)$$

where

$$f_0 = I_2 - C_3I_3 + C_4'I_2^2 + C_4I_4,\quad (5.1b)$$

and the scaled parameters are related to unscaled ones by

$$C_3 = \lambda^3\frac{C^{(3)}}{E_0}\ ; C_4' = \lambda^4\frac{C'^{(4)}}{E_0}\ ; C_4 = \lambda^4\frac{C^{(4)}}{E_0}.\ (5.2)$$

In spherical polar coordinates in OP space,

$$\vec{e} = (e_4, e_5, e_6) = \varepsilon(\sin\theta\cos\phi, \sin\theta\sin\phi, \cos\theta), \quad (5.3a)$$

with magnitude

$$\varepsilon \equiv |\vec{e}| = [{e_4}^2 + {e_5}^2 + {e_6}^2]^{1/2}. \quad (5.3b)$$

The invariants in OP space are then

$$I_2 = \varepsilon^2; \quad I_3 = \varepsilon^3 \sin^2\theta\cos\theta\sin\phi\cos\phi; I_4' = \varepsilon^4,$$

$$I_4 = \varepsilon^4[\sin^4\theta(\cos^4\phi + \sin^4\phi) + \cos^4\theta]. \quad (5.4)$$

Using trigonometric identities, f_0 is

$$f_0(\varepsilon,\theta,\phi) = \varepsilon^2 + C_4'\varepsilon^4 - \frac{C_3}{4}\varepsilon^3\sin\theta\sin 2\theta\sin 2\phi$$

$$+C_4\varepsilon^4[1 - \frac{1}{2}\sin^2 2\theta - \frac{1}{2}\sin^4\theta\sin^2 2\phi], \quad (5.5)$$

and has three remaining material constants C_3, C_4, C_4', while there are two scaling parameters λ, E_0.

The radial minimum $\partial f_0/\partial\varepsilon + 2(\tau-1)\varepsilon = 0$, and $\tau = 1$ degeneracy condition $f_0(\varepsilon = 1, \theta_m, \phi_m) = 0$ yield

$$C_3 = 6\sqrt{3}; \; {C_4}' = 1 - C_4/3, \quad (5.6)$$

achieved by the choice of scaling parameters

$$\lambda = \frac{(C^{(3)}/6\sqrt{3})}{[C'^{(4)} + (C^{(4)}/3)]}; \quad E_0 = \lambda^3\frac{C^{(3)}}{6\sqrt{3}}. \quad (5.7).$$

The angular minimum conditions $\partial f_0/\partial\phi = 0$, and $\partial f_0/\partial\theta = 0$ yield minima at $\cos 2\phi_m = 0$ or at

$$\sin 4\phi_m = 0, \quad 3\cos^2\theta_m = 1, \quad (5.8a)$$

$$\phi_m = (2m-1)\pi/N_V, \; m = 1,2,3,4(=N_V). \quad (5.8b)$$

For appropriate positive signs of the second derivatives, there are two points each on the northern and southern unit hemispheres in OP space,

$$\phi_m = \pi/4, 5\pi/4, \; \theta_m = \bar{\theta};$$

$$\phi_m = 3\pi/4, 7\pi/4, \; \theta_m = \bar{\theta} + \pi, \quad (5.9)$$

where $\cos\bar{\theta} = 1/\sqrt{3}$. These four minima $m = 1,2,3,4$ are at the ends of vectors in three-dimensional OP space $\vec{e} = \vec{e}_m \equiv \varepsilon_m(\sin\theta_m\cos\phi_m, \sin\theta_m\sin\phi_m, \cos\theta_m)$, that have equal relative separations or polyhedral sides of e.g. $|\vec{e_1} - \vec{e_2}| = 2\sqrt{2/3}\,\varepsilon_m$, and relative cosines of eg $\vec{e_1}.\vec{e_2}/\varepsilon_m^2 = \cos\psi = -1/3$, so the angle between vectors is the well-known tetrahedral angle $\psi = \cos^{-1}(-1/3) = 109^o28'$.

At transition, the Landau minima fall on the vertices and center of a tetrahedron, inscribed in a sphere of unit radius in $N_{OP} = 3$ dimensional order parameter space, as in the schematic points of Fig 3. The generic numbers for transition are in Table I. The maximum number of domain wall types is $N_W = 6$. Of course in this and other cases, this is only an upper bound, and energetic considerations might lead to fewer types actually appearing in the final microstructure.

Then the scaled Landau free energy in components is

$$\bar{f_L} = (\tau-1)I_2 + \{I_2 - 6\sqrt{3}I_3 + (1 - C_4/3)I_2^2 + C_4 I_4\}. \quad (5.10a)$$

In polar coordinates as in (2.23), it is

$$\bar{f}_L = [(\tau-1)\varepsilon^2 + \varepsilon^2(\varepsilon-1)^2] + \Delta f_0, \quad (5.10b)$$

manifestly showing the degeneracy at transition $\bar{f}_L(1, \theta_m, \phi_m) = 0$. The angular part $\Delta f_0 \equiv f_0(\varepsilon,\phi,\theta) - f_0(\varepsilon,\phi_m,\theta_m)$, is

$$\Delta f_0 = \frac{3\sqrt{3}}{4}\varepsilon^3[\frac{4}{3\sqrt{3}} - \sin\theta\sin 2\theta\sin 2\phi]$$

$$+C_4\varepsilon^4[\frac{2}{3} - \frac{1}{2}\sin^2 2\theta - \frac{1}{2}\sin^4\theta\sin^2 2\phi]. \quad (5.11)$$

This carries material dependence through C_4, but vanishes at minima, so $\bar{f}_L(\varepsilon,\theta_m,\phi_m)$ and hence $\bar{\varepsilon}(\tau)$ are still universal for all τ i.e. there is quasi-universality of the second kind. Here from (2.22d), $g_L = \tau - 1 + (\bar{\varepsilon} - 1)^2$.

The material-independent OP magnitude at the tetrahedron corners is

$$\bar{\varepsilon}(\tau) = \frac{3}{4}[1 + \sqrt{1 - 8\tau/9}], \quad (5.12)$$

and happens to be the same form as for the cubic/tetragonal transition, with the saddle-point barrier at $\bar{\varepsilon_b}(\tau) = \frac{3}{4}[1 - \sqrt{1 - 8\tau/9}]$. The Ginzburg term is $\bar{f}_G = \xi^2[\sum_{\ell=4,5,6}(\vec{\Delta}e_\ell)^2]$. The $n = 3$ non-OP strains are the compressional (e_1) and the deviatoric strains (e_2, e_3). The 3×3 compatibility kernel $U_{\ell\ell'}(\vec{k})$ of (2.19) is given in (A20).

B. Square/oblique case : $N_V = 4, N_{OP} = 2, n = 1$

A square converts to an unequal-sided oblique polygon with the deviatoric e_2, and shear e_3 order parameters acting simultaneously. Since each can distort the square in two ways, one expects four variants, as in Fig 1. The harmonic parts are assumed to soften at the same T_c (otherwise they would be two

separate, unrelated transitions). The joint action of the two order parameters is through their coupling. The square point group G= $p4mm$ with $\nu_G = 4$ goes to g = $p2$ with $\nu_g = 1$, so there are[15] $N_V = 4$ variants, as expected. The anharmonic invariants are as in the square/rectangle case, e_2^4, e_2^6 and e_3^4, e_3^6 or $p_{max} = 6$ separately for each OP. We consider the simplest case of equal elastic constants, and the simplest coupling $e_2{}^2 e_3^2$. The scaled free energy term f_0 is:

$$f_0 = (e_2^2+e_3^2) - C_4(e_2^4+e_3^4) + C_6(e_2^6+e_3^6)] - C_4' e_2{}^2 e_3{}^2, \ (5.13)$$

where the scaled and unscaled coefficients are related by $C_4 = C^{(4)}\lambda^4/E_0$; $C_6 = C^{(6)}\lambda^6/E_0$; $C_4' = C'^{(4)}\lambda^4/E_0$.

Transforming to polar coordinates $(e_2, e_3) = \varepsilon(\cos\phi, \sin\phi)$, with $\eta_2 \equiv \cos 2\phi$, and using trigonometric identities, this becomes

$$f_0 = t_0(\varepsilon) + t_4(\varepsilon)\eta_2{}^2, \quad (5.14)$$

where the coefficients are

$$t_0 \equiv \varepsilon^2 - \frac{\varepsilon^4}{4}(2C_4 + C_4') + \frac{\varepsilon^6}{4}C_6, \quad (5.15a)$$

$$t_4 \equiv \frac{3}{4}C_6\varepsilon^6 - \frac{(2C_4 - C_4')\varepsilon^4}{4}. \quad (5.15b)$$

The angular dependence is $f_0 \sim \cos 4\phi$. The degeneracy condition, and the radial minimum condition at transition finally yield $C_4 + C_4'/2 = 4$; $C_6 = 4$, achieved through the choice

$$\lambda^2 = (C^{(4)} + C'^{(4)}/2)/C^{(6)}; \ E_0 = \lambda^6 C^{(6)}/4. \ (5.16)$$

The angular minima are at $\eta_2(\phi_m)^2 = 1$ or

$$\sin 4\phi_m = 0; \ \phi_m = \frac{(2m-1)\pi}{N_V}, \ m = 1, 2, 3, 4(= N_V). \ (5.17)$$

Then the scaled free energy in OP components is

$$f_0 = \bar{e}^2 - (4 - \frac{1}{2}C_4')(e_2^4+e_3^4) + 4(e_2^6+e_3^6) - C_4' e_2{}^2 e_3{}^2. \ (5.18a)$$

In polar coordinates as in (2.23),

$$\bar{f}_L = [(\tau-1)\varepsilon^2 + \varepsilon^2(\varepsilon^2-1)^2] + \Delta f_0,$$

$$\Delta f_0 = \varepsilon^4(3\varepsilon^2 - 2 + C_4'/2)\cos^2 2\phi, \quad (5.18b)$$

so the quasi-universality is of the second kind, with $\bar{f}_L(\varepsilon, \phi_m)$ and $\bar{\varepsilon}(\tau)$ of (3.6), both independent of material constants. Here $g_L = \tau - 1 + (\bar{\varepsilon}^2 - 1)^2$.

At transition, the $N_V = 4$ variant minima fall on the vertices of a square inscribed in a unit circle in $N_{OP} = 2$ dimensional order parameter space. These are the only variants for $C_4' > 1$, as the trivial roots on the axes $(e_2, e_3) = (\pm\bar{\varepsilon}, 0), (0, \pm\bar{\varepsilon})$ are then unstable. The maximum possible number of domain wall types is $N_W = N_V(N_V-1)/2 = 6$.

The Ginzburg term is $f_G = \xi^2[(\vec{\Delta}e_2)^2 + (\vec{\Delta}e_3)^2]$. There is a single $n = 1$ non-OP variable e_1 as in the triangle-centered rectangle case, so the compatibility kernel from the compressional harmonic term e_1^2 is the same as the 2×2 matrix $U_{\ell\ell'}$ of (A2).

VI. TRANSITIONS WITH $N_V = 6$

We consider two transitions with $N_V = 6$ variants, and $N_{OP} = 2$ order parameters (OP), but with different numbers n of non-OP strains. They are the (a) cubic/orthorhombic case in 3D ($n = 4$); and (b) triangle/center rectangle case in 2D ($n = 1$). See Figs 1 and 2.

A. Cubic/orthorhombic case $N_V = 6, N_{OP} = 2, n = 4$

For a cubic to orthorhombic distortion, the cross-sectional area perpendicular to each of three axes can be rectangular in two ways, so one expects six variants, as in Fig 2. The symmetry group G = $Pm\bar{3}m$ with $\nu_G = 48$ elements goes to the orthorhombic group g = $Pmmm$ with $\nu_g = 8$ elements, so[6] $N_V = 48/8 = 6$, as expected. The variants are generated by combined action of the $N_{OP} = 2$ order parameter components that are the two 3D deviatoric strains, with the vector in OP space chosen as in the cubic/ tetragonal case, $\vec{e} = (e_3, e_2) \sim (\frac{1}{\sqrt{6}}\{X^2+Y^2-2Z^2\}, \frac{1}{\sqrt{2}}\{X^2-Y^2\})$.

The cubic/orthorhombic free energy in Cartesian strains has been considered for fitting to FePd experiments[7]; here however, we work with physical strains. The previous cubic/tetragonal case of (4.1), with a third order invariant $I_3 = e_3{}^3 - 3e_3 e_2{}^2$, yielded three minima alternating with three maxima, on the unit circle. For six minima on the unit circle, a sixth order invariant $I_6 = I_3^2$ will be the leading angular term.

We consider two cases, with up to sixth order, and up to eighth order invariants. For invariants of up to $p_{max} = 6$th order, the free energy has $N_{max} = 4$ material coefficients. $\bar{f}_L = (\tau-1)(e_3^2+e_2^2) + f_0(e_3, e_2)$ where f_0 is

$$f_0 = I_2 - C_4 I_2^2 - C_6 I_6 + C_6' I_2^3, \ (6.1a)$$

with signs $\sigma_4 = \sigma_6 = -1, \sigma_6' = +1$. For materials with other coefficient signs, we are forced to go to higher $p_{max} = 8$th order, and the additional invariants are $I_8 = I_3^2 I_2, I_8' = I_2^4$. (The odd invariants $I_3, I_5 = I_3 I_2, I_7 = I_5 I_2$ give sign-varying contributions to derivatives $\partial f_0/\partial\phi$ at different minima that should be equivalent, so we set their coefficients to zero from the start.)

The scaled free energy up to eighth order, with $N_{max} = 6$ material coefficients is

$$f_0 = I_2 - C_4 I_2^2 + C_6 I_6 - C_6' I_2^3 - C_8 I_8 + C_8' I_2^4. \ (6.1b)$$

It is convenient to define ${C_6}^{(-)} \equiv C_6' - C_6, {C_8}^{(-)} \equiv C_8' - C_8$. Transforming to polar coordinates, $\vec{e} = (e_3, e_2) = \varepsilon(\cos\phi, \sin\phi)$ we get $I_3 = \varepsilon^2 \cos 3\phi$ as before, so $I_6 = \varepsilon^6 \eta_3^2, I_8 = \varepsilon^8 \eta_3^2$ where $\eta_3 \equiv \cos 3\phi$.

Collecting terms, the sixth and eighth order cases of (6.1a) and (6.1b) can both be written as

$$f_0 = t_0(\varepsilon) + t_6(\varepsilon)(1 - \eta_3^2), \ \ (6.2)$$

where from (6.1a)

$$t_0 \equiv \varepsilon^2 - C_4 \varepsilon^4 + {C_6}^{(-)} \varepsilon^6; \ t_6 \equiv C_6 \varepsilon^6; \ (6.3a)$$

while from (6.1b),

$$t_0 \equiv \varepsilon^2 - C_4 \varepsilon^4 - {C_6}^{(-)} \varepsilon^6 + {C_8}^{(-)} \varepsilon^8; \ t_6 \equiv C_8 \varepsilon^8 - C_6 \varepsilon^6. \ (6.3b)$$

In both cases, the angular dependence is $f_0 \sim -\cos 6\phi$.

For the sixth order case of (6.3a), the degeneracy $f_0(\varepsilon = 1, \phi = \phi_m) = 0$ and radial minimum condition $\partial f_0/\partial \varepsilon + 2(\tau - 1)\varepsilon = 0$ determine two of the constants as ${C_6}^{(-)} = 1, C_4 = 2$. The scaling parameters for these values are, with unscaled elastic-coefficient ratio $\alpha \equiv C^{(4)}/(C'^{(6)} - C^{(6)})$,

$$\lambda^2 = \alpha/2, \quad E_0 = \lambda^4 C^{(4)}/2. \ (6.4)$$

Then the angular contributions clearly yield $\partial f_0/\partial \phi = 0$ roots at

$$\sin 6\phi_m = 0; \ \phi_m = \frac{2(m-1)\pi}{N_V}, \ m = 1, ...6 (= N_V). \ (6.5)$$

where ${\eta_3(\phi_m)}^2 = 1$.

The scaled free energy in components in OP space is, with the above scaled coefficients,

$$\bar{f_L} = (\tau - 1) I_2 + I_2 (I_2 - 1)^2 + C_6 ({I_2}^3 - {I_3}^2). \ (6.6)$$

In polar coordinates as in (2.23),

$$\bar{f_L} = [(\tau - 1)\varepsilon^2 + \varepsilon^2 (\varepsilon^2 - 1)^2] + \Delta f_0,$$

$$\Delta f_0 = \frac{1}{2} C_6 \varepsilon^6 (1 - \cos 6\phi), \quad (6.7)$$

The last term Δf_0 vanishes at the six minimal directions, where the material constant C_6 is eliminated, so there is quasi-universality of the second kind. The OP magnitude $\bar{\varepsilon}(\tau)$ is as in the tetragonal/orthorhombic case of (3.6). The variants are manifestly degenerate with austenite as $\bar{f_L}(1, \phi_m) = 0$ at transition.

For the eighth order case of (6.3b), there are three material constants $C_4, {C_6}^{(-)}, {C_8}^{(-)}$ in $\bar{f_L}(\varepsilon, \phi_m)$, and only two remaining scaling parameters λ, E_0. The degeneracy and radial minimum condition now determine two of the constants as ${C_6}^{(-)} = 3 - 2C_4, {C_8}^{(-)} = 2 - C_4$. The equivalent condition $3{C_8}^{(-)} - 2{C_6}^{(-)} - C_4 = 0$, yields with (2.12), a quadratic, $3\lambda^4 - 2\gamma\lambda^2 - \alpha\gamma$, where α is as above and $\gamma \equiv (C'^{(6)} - C^{(6)})/(C'^{(8)} - C^{(8)})$. The positivity of second derivatives requires that $C_8 > C_6$ and $2 - C_4 > 0$ while $\lambda^2 > 0$ below, further requires $3 - 2C_4 > 0$.

However $\lambda (\ll 1)$ can also be obtained from the relation between scaled and unscaled coefficients (2.12), as $\lambda^2 = \alpha(3 - 2C_4)/C_4 = \gamma(2 - C_4)/(3 - 2C_4)$. Demanding consistency yields λ, E_0, C_4 in terms of the unscaled elastic coefficients, but here C_4 is no longer just a universal number. The scaling parameters are then

$$\lambda = (\gamma/3)[1 + \{1 + 3\alpha/\gamma\}^{1/2}]; \ \ E_0 = C^{(4)} \lambda^4 / C_4; \ \ (6.8a)$$

$$C_4 = (3/2)/[1 + (\gamma/6\alpha)(1 + \{1 + 3\alpha/\gamma\}^{1/2})]. \ (6.8b)$$

As elastic constants vary, the constant $C_4(\alpha/\gamma)$ moves in a narrow range $3/2 > C_4 > 0$, e.g. $C_4 = 1$ for $\alpha/\gamma = 1$.

The scaled free energy in OP components for the eighth order case from (6.3b) is then

$$\bar{f_L} = (\tau - 1) I_2 + I_2 (I_2 - 1)^2 \{1 + (2 - C_4) I_2\}$$

$$+ (C_8 I_2 - C_6)({I_2}^3 - {I_3}^2). \ \ (6.9)$$

In polar coordinates as in (2.23),

$$\bar{f_L} = [(\tau - 1)\varepsilon^2 + \varepsilon^2 (\varepsilon^2 - 1)^2 \{1 + (2 - C_4)\varepsilon^2\}] + \Delta f_0,$$

$$\Delta f_0 = \frac{1}{2} (C_8 \varepsilon^8 - C_6 \varepsilon^6)(1 - \cos 6\phi). \quad (6.10)$$

with C_8, C_6 eliminated at minimal angular directions.

The root $\bar{\varepsilon}(\tau)$ is the solution of a cubic

$$4(2 - C_4) X^3 + 3(5 - 2C_4) X^2 + 2(3 - C_4) X + (\tau - 1) = 0, \ (6.11)$$

where $X \equiv \bar{\varepsilon}^2 - 1 \geq 0$. At $\tau = 1$, the required root is $X = 0$, and just below transition is linear, $X \simeq (1 - \tau)/2(3 - C_4)$. Close to zero temperature, with $\tau = -|\tau|$ and for $|\tau(T = 0)| = T_c/(T_0 - T_c) >> 1$, one has $X \simeq [|\tau|/4(2 - C_4)]^{1/3}$. Thus the scaling procedure carries through even for the eighth order case, but there is now quasi-universality of the third kind, with a weak residual material-dependence through C_4.

At transition and for both cases, the $N_V = 6$ nontrivial Landau minima fall on the vertices of a hexagon[7] inscribed in a unit sphere in $N_{OP} = 2$ order-parameter space as in Fig.

3 and Table I. The upper bound on the number of possible martensite-martensite domain wall types is $N_W = N_V(N_V - 1)/2 = 15$, although as mentioned, not all of these may be seen, for energetic reasons.

The Ginzburg term, and the compatibility potential from the $n = 4$ non-OP harmonic term is the same as in the cubic/tetragonal case of (A23) of the Appendix.

B. Triangle/oblique case $N_V = 6, N_{OP} = 2, n = 1$

The two order parameter components are the single deviatoric and single shear strains, $\vec{e} = (e_2, e_3) = \varepsilon(\cos\phi, \sin\phi)$. The triangle point group G = $p6mm$ with $\nu_G = 6$ goes to the subgroup g =$p2$ with $\nu_g = 2$ so there are[15] $N_V = \nu_G/\nu_g = 6$ variants. (The ratio of the numbers of rotational elements would however give $3/1 = 3$ variants.)

The scaled Landau free energy density[13] is formally similar to the cubic/orthorhombic case of (6.7). At transition the $N_V + 1 = 6 + 1$ degenerate Landau minima again fall on the six vertices and at the center of a hexagon inscribed in a unit circle, as in Fig 2. The maximum number of domain wall types is $N_W = 15$, but not all may finally appear.

The Ginzburg term, and the compatibility potential from the $n = 1$ non-OP harmonic term is the same as in the triangle/centered rectangle case of (A2).

VII. PSEUDOSPIN HAMILTONIANS

The idea of using discrete-variable pseudospins to approximate continuous-variable distortions on a lattice was proposed earlier[20,21], and has been pursued[22–25]. We had suggested obtaining pseudospin hamiltonians for various transitions by substituting the order parameter (OP) values at the polar coordinate Landau minima, into the total scaled free energy[22]. The $N_{OP} = 1$ case for the square/rectangle case as $e_2(\vec{r}) \to \bar{\varepsilon}S(\vec{r})$, where the three minima induce a spin-1 model $S = 0, +1, -1$ with three values on a line, of a single-component pseudospin. With $S^6 = S^4 = S^2 = 1$ or 0, the nonlinearities in the Landau free energy collapse to $\bar{f}_L \to \bar{\varepsilon}(\tau)^2 g_L(\tau) S^2$ where $g_L(\tau) = \tau - 1 + (\bar{\varepsilon}^2 - 1)^2$ changes sign at transition. The Ginzburg and compatibility terms are also written in terms of pseudospins. This yields a temperature-dependent pseudospin hamiltonian $H(S) \equiv F(e_2 \to \bar{\varepsilon}S)$ that is like a generalized Blume-Capel spin-1 model[19]. The hamiltonian has a temperature-dependent quadratic term, a nearest-neighbor ferromagnetic term, and a PLA compatibility term[23],

$$\beta H(S) = \frac{D_0}{2}[\sum_{\vec{r}}\{g_L S^2(\vec{r}) + \xi^2(\vec{\Delta}S)^2\}$$

$$+ \sum_{\vec{r},\vec{r}'} \frac{A_1}{2} U(\vec{r} - \vec{r}')S(\vec{r})S(\vec{r}')], \quad (7.1)$$

with gradient $\vec{\nabla}$ realized as difference operators $\vec{\Delta}$ on a computational grid, as mentioned. Here $D_0(T) \equiv 2\bar{\varepsilon}^2(\tau)E_0/k_BT$, and the hamiltonian is diagonal in Fourier space,

$$\beta H = \frac{1}{2}\sum_{\vec{k}} Q_0(\vec{k})|S(\vec{k})|^2; \quad (7.2a)$$

$$Q_0(\vec{k}) \equiv D_0[g_L(\tau) + \xi^2\vec{K}^2 + \frac{A_1}{2}U(\vec{k})]. \quad (7.2b)$$

Here on a grid of unit lattice constant, $K_\mu \equiv 2\sin(k_\mu/2)$, with $\mu = x, y$. This hamiltonian has been studied in a local meanfield approximation, under a cooling ramp obtaining glassy domain-wall textures, dependent on cooling rate and initial conditions[23].

For $N_{OP} > 1, N_V > 2$ transitions we *do not* simply get a generalized spin-j model with $2j + 1$ states on a line, where $j = N_V/2$. Instead we obtain clock-like models[19] with discrete $\vec{S}$ vector variables pointing to $N_V + 1$ corners and centre of a polyhedron in N_{OP}-dimensional space, as denoted by arrows in Fig. 3. Since the zero state is included, these may be termed 'clock-zero' $\mathbb{Z}_{N_V+1}$ models. Note that, unlike pure clock $\mathbb{Z}_N$ models, the spin square-magnitude $\vec{S}^2(\vec{r})$ is still a statistical variable and not a constant, because of the zero states. Choosing $N_{OP} = 2, 3$ component strains only at the minima induces vector pseudospins in OP space,

$$\vec{e}(\vec{r}) \to \bar{\varepsilon}\vec{S}(\vec{r}). \quad (7.3)$$

The variant angular dependence $\bar{f}_L \sim -\cos N_V\phi$ generates the clock-variable directions.

The general temperature-dependent pseudospin hamiltonian is

$$H(S_\ell(\vec{r})) = F(e_\ell \to \bar{\varepsilon}S_\ell). \quad (7.4)$$

As in the square/rectangle case, the radial part of the Landau term with OP nonlinearities, collapses to a quadratic in the pseudospin magnitude, since nth powers of the spin-vector magnitude $|\vec{S}|^n = |\vec{S}|^2 = 0, 1$.

Although in zero stress the uniform state is no longer a Landau minimum below the lower spinodal T_c, there is a possibility that nonuniform textures exert local internal stresses to favor the zero value at a site even at low temperatures. Also, the original free energy in OP strain always has a turning point at the origin to support dynamical transient zeros, that although few in number, could play a catalytic role in microstructural evolution[23]. Hence we retain zero spin values at all temperatures, allowing their permanent/transient existence to be determined dynamically.

The hamiltonian in coordinate space is

$$\beta H = \frac{D_0}{2}[\sum_{\vec{r},\ell}\{g_L(\tau)S_\ell(\vec{r})^2 + \xi^2(\vec{\Delta}S_\ell)^2\}$$

$$+ \sum_{\vec{r},\vec{r}',\ell,\ell'} \frac{A_1}{2} U_{\ell\ell'}(\vec{r}-\vec{r}') S_\ell(\vec{r}) S_{\ell'}(\vec{r}')], \quad (7.5a)$$

and is transition-specific through the $\vec{S}$ values, the temperature dependence of $g_L(\tau)$, and the compatibility potential. Note that the anisotropic terms $\vec{S}(\vec{r}).\overleftrightarrow{U}(\vec{r}-\vec{r}').\vec{S}(\vec{r}')$ are from compatibility anisotropies in OP space, and differ from models with electric dipoles $\vec{d}$ that have anisotropies relative to coordinate space axes[24] $\{\vec{d}(\vec{r}).\hat{r}\}\{\vec{d}(\vec{r}').\hat{r'}\}/|\vec{r}-\vec{r'}|^d$, (although the powerlaw fall-offs with exponent d, are the same).

The hamiltonian is diagonal in Fourier space,

$$\beta H = \frac{1}{2} \sum_{\vec{k}} \sum_{\ell,\ell'} Q_{0,\ell\ell'}(\vec{k}) S_\ell(\vec{k}) S_{\ell'}(\vec{k})^*; \quad (7.6a)$$

$$Q_{0,\ell\ell'}(\vec{k}) \equiv D_0[\{g_L(\tau) + \xi^2 \vec{K}^2\}\delta_{\ell,\ell'} + \frac{A_1}{2} U_{\ell\ell'}(\vec{k})]. \quad (7.6b)$$

Transitions with free energy quasi-universality of the first and second kind, have reduced pseudospin hamiltonians with *universal* coefficients g_L of the on-site term. Apart from the overall E_0, the material-dependence is only through the texture-inducing Ginzburg and St Venant terms.

For two-component OP cases in addition to $\vec{S} = 0$, the pseudospin is $\vec{S} = (\cos\phi_m, \sin\phi_m)$, where m takes on N_V values. Thus for the three variants of the cubic/tetragonal and triangle/center-rectangle transition, there are three values $\phi_m = 0, 2\pi/3, 4\pi/3$ on corners of a triangle, and $g_L = \tau - 1 + (\bar{\varepsilon} - 1)^2$ where $\bar{\varepsilon}(\tau)$ is from (4.9). The four spin vectors are $\vec{S} = (0,0), (1,0), (-\frac{1}{2}, \pm\frac{\sqrt{3}}{2})$.

For the square/oblique transition there are four values $\phi_m = \pi/4, 3\pi/4, 5\pi/4, 7\pi/4$ on corners of a square, and $g_L = \tau - 1 + (\bar{\varepsilon}^2 - 1)^2$, with $\bar{\varepsilon}(\tau)$ of (3.6). The five spin vectors are $(0,0), (\pm\frac{1}{\sqrt{2}}, \frac{1}{\sqrt{2}}), (\pm\frac{1}{\sqrt{2}}, -\frac{1}{\sqrt{2}})$.

For the three-component OP of the cubic/trigonal transition, the pseudospin vectors are *non-planar* as $\vec{S} = (\sin\theta_m \cos\phi_m, \sin\theta_m \sin\phi_m, \cos\theta_m)$, where θ_m, ϕ_m take on four values of (5.8) at the corners of a tetrahedron. The coefficient $g_L = \tau - 1 + (\bar{\varepsilon} - 1)^2$, with $\bar{\varepsilon}(\tau)$ the same as the cubic/tetragonal case of (4.9). The five spin vectors are $(0,0,0), (\pm\frac{1}{\sqrt{3}}, \pm\frac{1}{\sqrt{3}}, \frac{1}{\sqrt{3}}), (\pm\frac{1}{\sqrt{3}}, \mp\frac{1}{\sqrt{3}}, -\frac{1}{\sqrt{3}})$.

For the two-component OP and six variants of the cubic/orthorhombic and triangle/oblique transitions, $\phi_m = 0, \pi/6, 2\pi/6, ..., 5\pi/6$ on the six corners of a hexagon, and the seven spin vectors are $(0,0), (\pm 1, 0), (\frac{1}{2}, \pm\frac{\sqrt{3}}{2}), (-\frac{1}{2}, \pm\frac{\sqrt{3}}{2})$, where for the $p_{max} = 6$ case, $g_L(\tau) = \tau - 1 + (\bar{\varepsilon}^2 - 1)^2$ is universal, and $\bar{\varepsilon}(\tau)$ as in (3.6). For the $p_{max} = 8$ case, with quasi-universality of the third kind, there is a weak material-dependence through $g_L = \tau - 1 + (\bar{\varepsilon}^2 - 1)^2[1 + \bar{\varepsilon}^2(2 - C_4)]$ with $3/2 > C_4 > 0$, and $\bar{\varepsilon}(\tau)$ as in (6.11).

The pseudospin reduced hamiltonians here are not just written down, but are induced from the scaled free energy, that encodes the specific symmetry, nonlinearity, and compatibility of each ferroelastic transition: a continuum-variable materials science model is mapped to a discrete-variable statistical mechanics hamiltonian.

VIII. SIMULATIONS OF STRAIN TEXTURES

Spatially varying strain textures in ferroelastics can be numerically simulated in continuous strains by free energy relaxations, or by discrete-strain pseudospin hamiltonians.

A. Scaled free energy relaxations

Of course, there has been much simulation work in the displacement representation or with phase fields[28], and one common problem is the choice of the many N_{mat} material coefficients, that require fitting to experiment for each material[7]. With scaled free energy strain dynamics or with pseudospin hamiltonians, the material-dependence is essentially eliminated or reduced, to group many materials with the same structural transition in the same quasi-universality class. Thus one does not have to explore the full many-parameter space of N_{mat} unscaled coefficients, and simulations by different groups can be more easily compared.

Local equilibrium microstructures can be found from relaxational dynamics of unscaled order parameter (OP) strains, $\{e'_\ell(r,t)\}$ and the unscaled free energies: $\partial e'_\ell/\partial t = -\Gamma^{(0)} \partial F/\partial e'_\ell$, where $\Gamma^{(0)}$ is a kinetic constant of dimension inverse-energy $\times$ time. Scaling strains, $e'_\ell = \lambda e_\ell$ and energies $F = E_0 \bar{F}$, where $\bar{F} = \bar{F}_L + \bar{F}_G + \bar{F}_{compat}$, we obtain a characteristic decay rate $\Gamma_0 \equiv \Gamma^{(0)} E_0/\lambda^2$. Then with a dimensionless time $\bar{t} \equiv \Gamma_0 t$ absorbing E_0, a scaled dimensionless dynamics is obtained,

$$\frac{\partial e_\ell}{\partial \bar{t}} = -\frac{\partial \bar{F}(e_\ell)}{\partial e_\ell}. \quad (8.1)$$

The underdamped dynamics[13] could be similarly scaled to quasi-universal, dimensionless form.

B. Pseudospin simulations

Microstructures can be studied using pseudospin hamiltonians, by solving self-consistency equations from local meanfield approximations and by Monte Carlo spin simulations[29].

1. *Local meanfield*

The completely uniform $\vec{k} = 0$ meanfield contribution to the hamiltonian is $H \sim f_L(\tau)\vec{S}^2(\vec{k} = 0)$, as the Ginzburg and compatibility terms vanish. Thus as $\bar{f}_L = \bar{\varepsilon}^2 g_L$ changes sign at transition, we have $< S^2 >= 0$ above the transition, and $< S^2 >= 1$ below the transition, faithfully reproducing the displacive transition of the original strain variable[23]. Strain textures with $\vec{k} \neq 0$, can be captured by *local* meanfield $\sigma_\ell(\vec{r}) \equiv < S_\ell(\vec{r}) >$ approximations in both coordinate and Fourier space. Each spin sees a local meanfield, and there is a subtraction for consistency of averages $< SS > \simeq \sigma\sigma$:

$$S_\ell(\vec{r})S_{\ell'}(\vec{r}') \to S_\ell(\vec{r})\sigma_{\ell'}(\vec{r}') + \sigma_\ell(\vec{r})S_{\ell'}(\vec{r}')$$

$$-\sigma_\ell(\vec{r})\sigma_{\ell'}(\vec{r}') \quad (8.2a)$$

$$S_\ell(\vec{k})S_{\ell'}(\vec{k})^* \to S_\ell(\vec{k})\sigma_{\ell'}(\vec{k})^* + \sigma_\ell(\vec{k})S_{\ell'}(\vec{k})^*$$

$$-\sigma_\ell(\vec{k})\sigma_{\ell'}(\vec{k})^*. \quad (8.2b)$$

This is equivalent to substituting $S = \sigma + \delta S$ into the hamiltonian, and linearizing in $\delta S \equiv S - \sigma$.

The meanfield hamiltonian is then,

$$\beta H_{MF} = \sum_{\ell,\vec{r}} Q_\ell(\vec{r})S_\ell(\vec{r}) = \sum_{\ell,\vec{k}} Q_\ell(\vec{k})^* S_\ell(\vec{k}), \quad (8.3)$$

where an additive constant $-\frac{1}{2}\sum_{\vec{r}} Q_\ell(\vec{r})\sigma_\ell(\vec{r})$ on the right is suppressed. Here $Q_\ell(\vec{r}) \equiv \sum_{\ell',\vec{r}'} Q_{0,\ell\ell'}(\vec{r}-\vec{r}')\sigma_{\ell'}(\vec{r}')$, or $Q_\ell(\vec{k}) \equiv \sum_{\ell'} Q_{0,\ell\ell'}(\vec{k})\sigma_{\ell'}(\vec{k})$. The same results are obtained from a $\vec{k} \neq 0$ variational approach in the weights $\rho(\vec{k})$, minimizing $Trace(H\rho) - \sum_{\vec{k}} \rho(\vec{k}) \ln \rho(\vec{k})$, that has averages such as $\sigma_\ell(\vec{k}) = Trace\{\rho(\vec{k})S(\vec{k})\}$.

The self-consistency condition for the local, nonuniform meanfield is then

$$\sigma_\ell(\vec{r}) = \sum_{S_\ell} S_\ell(\vec{r}) e^{-\beta H_{MF}} / [\sum_{S_\ell} e^{-\beta H_{MF}}]. \quad (8.4).$$

For the $N_{OP} = 1, N_V + 1 = 3$ square/rectangle case, one obtains[23]

$$\sigma(\vec{r}) = -2\sinh Q(\vec{r}) / [1 + 2\cosh Q(\vec{r})]. \quad (8.5).$$

2. *Monte Carlo simulations*

Metropolis algorithms for nearest-neighbor Ising models with spin components $N_{OP} = 1$ and values $N_V = 2$, are prototypical. The Monte Carlo method can be applied to spins of $N_{OP} = 1, 2, 3$ components, with $N_V + 1 = 3, 4, 5, 7$ values and powerlaw anisotropic interactions. Fast Fourier Transforms (FFT) are used to easily treat the full PLA compatibility potentials; this is preferable to attempting an uncontrolled truncation of the $1/R^d$ interactions to some arbitrarily far-neighbor interaction, while staying only in coordinate space. The procedure is:

(i) Flips of an input spin configuration with an input energy H_{input} are made on the lattice in coordinate space, with equal probability over *all* $N_V + 1$ values at a site, yielding a trial new configuration $\{\vec{S}(\vec{r})\}$.

(ii) An FFT gives the Fourier space $\{\vec{S}(\vec{k})\}$.

(iii) The trial energy H_{trial} (diagonal in Fourier space as in (7.6b)) is then evaluated. The energy difference $\Delta H = H_{trial} - H_{input}$ between configurations in the Boltzmann-factor $e^{-\beta\Delta H}$, determines the accepted configuration. The cycle then repeats.

The N sites are labelled with random numbers and arranged in an increasing-value chain, so sequentially visiting every site in the chain means every site is visited randomly, but once and only once, in 1 MC sweep, that then corresponds to 1 MC step per spin.

IX. SUMMARY

Generalizing a procedure due to Barsch and Krumhansl, we have shown that ferroelastic free energies can be scaled in dimensionless form, defining a quasi-universality class for all materials with the same group/subgroup structural transition. Whereas unscaled free energies with fitted coefficients are specific to the fitted material[7], the scaled dimensionless free energies are in a form relevant for all materials with the same ferroelastic transition. A simplifying approximation works to leading order in the (unscaled) spontaneous- strain magnitude at transition λ, that is typically a few percent. To this order, the scaled Landau free energy minima turn out in most cases to be material-independent, depending only on the dimensionality d, number of order parameter components N_{OP}; and number of low-temperature structural variants N_V. The minima in order-parameter space fall on the corners of 'polyhedra' inscribed in 'spheres' in N_{OP} dimensions, with radius the scaled order parameter magnitude, that is unity at transition. The scaled variational free energies in terms of the local order-parameter strain components, have Landau, Ginzburg, and St Venant powerlaw anisotropic interactions, and can be used in relaxational or underdamped dynamic simulations. The compatibility kernels are calculated for all transitions considered, using a constraint-substitution method.

The polyhedral arrangement of minima in the strain variables immediately suggests a reduced description with strain free energies inducing 'clock-zero' models, with N_{OP}-dimensional discrete pseudospin vectors at each site, pointing to $N_V + 1$ possible states. The discrete-variable pseudospins in local meanfield and Monte Carlo simulations can be shown[29] to reproduce previous textures obtained in continuous-variable dynamics[11–14,28].

Further work could include pseudospin clock-zero simulations of more of the transitions considered here; the addition of quenched disorder; a determination[7,15] of the scaled free energies and compatibility kernels for more of the 94 possible ferroelastic transitions[6]; scaling of experimental results for different materials to explore data clustering; and simulating complex oxide models, through couplings of strains to other fields[17].

This work was supported in part by the U.S. Department of Energy, and by ICTP, Trieste.

X. APPENDIX: ST VENANT COMPATIBILITY KERNELS FOR FERROELASTIC TRANSITIONS

We derive in this Appendix, the Fourier space compatibility kernels, for increasing numbers n of non-order parameter strains: $n = 1, 2$ for 2D transitions, and $n = 3, 4, 5$ for 3D transitions.

The background for compatibility ideas includes the following. Kartha et al[11] performed Monte Carlo simulations in the displacement-vector representation, using a square/rectangle variational free energy $F(\vec{\nabla}\vec{u})$ that, in addition to a Landau term nonlinear in the order parameters (OP), also included harmonic terms in compression and shear $\sim (\nabla_x u_x + \nabla_y u_y)^2$ and $\sim (\nabla_y u_x + \nabla_x u_y)^2$. They found diagonal domain walls. To understand the orientation, they followed Baus and Lovett[10] and went over to the strain representation, analytically minimizing these non-OP $\sim {e_1}^2, {e_3}^2$ terms subject to the St Venant constraint using Lagrange multipliers. The resultant square/ rectangle compatibility kernel explained the $\pi/4$ orientation preference. However, strain-representation simulations in the OP e_2, for a free energy $F(e_2)$ that explicitly included the St Venant term, were not pursued. This changeover to the OP-strain working variable was done in relaxational simulations[12], yielding the same diagonal domains. Strain-variable simulations using compatibility kernels for other 2D cases[13,15], and the 3D cubic/tetragonal case[14], found textures as obtained in the displacement and phase-field representations[28]; and an underdamped strain dynamics including compatibility potentials was proposed, including Langevin dynamics noise terms with powerlaw spatial correlations[13].

Here we pursue this strain-representation project, contributing to a catalog of 3D ferroelastic $N_{OP} \times N_{OP}$ matrix kernels that incorporate the three compatibility constraints (2D kernels for ferroelastic transitions were previously given in[15]). Instead of using, and solving for, three Lagrange multipliers, we directly solve the constraints in Fourier space for three non-OP strains, and substitute in the harmonic non-OP free energies, followed by an unconstrained minimization in any remaining non-OP strains[17]. The four 3D transitions have three distinct kernels, that are plotted in Fig 4. As a check, we apply the direct substitution method to find 2D kernels, previously obtained by Lagrange multipliers[11–15]. In Fourier space derivatives go as eg ${\nabla_\mu}^2 \to -{k_\mu}^2$, while on a grid with difference operators ${\Delta_\mu}^2 \to -{K_\mu}^2$ where $K_\mu \equiv 2\sin(k_\mu/2)$. Here in compatibility equations we write for simplicity just the wave vectors like k_μ, with the understanding that they can be replaced by K_μ in grid simulations.

The compatibility constraint in minimizing the harmonic non-OP terms $\bar{f}_{non} = \sum_i (A_i/2)|e_i(\vec{k})|^2$ only affects *nonuniform* strains with nonzero wave-vector. The uniform or zero wavevector parabolic terms are freely minimized by zero values, $e_i(\vec{k} = 0) = 0$. Thus a prefactor of $\nu(\vec{k}) \equiv 1 - \delta_{\vec{k},0}$ must be inserted in the results below for the kernels. The resultant sign-varying compatibility potentials have zero spatial average $< U(\vec{R}) > \sim U(\vec{k} = 0) \sim \nu(\vec{k} = 0) = 0$, rather than a divergence as for isotropic potentials $< U(R) > \sim \sum_{\vec{R}} 1/R^d \sim \ln N$.

A. 2D transitions

In 2D, the Fourier constraint of (2.3b) in terms of Cartesian distortions is $2k_x k_y e_{xy} - {k_y}^2 e_{xx} - {k_x}^2 e_{yy} = 0$. In terms of physical strains of (2.5) and with only one shear $s = 3$, this becomes the single compatibility constraint as in (2.7),

$$O_1 e_1 + O_2 e_2 + O_3 e_3 = 0. \ (A1)$$

For the square lattice, the compatibility coefficients are $O_1(\vec{k}) = -\frac{1}{\sqrt{2}}\vec{k}^2, O_2(\vec{k}) = +\frac{1}{\sqrt{2}}({k_x}^2 - {k_y}^2), O_3(\vec{k}) = 2k_x k_y$, while for the triangular case,$O_1(\vec{k}) = -\vec{k}^2, O_2(\vec{k}) = ({k_x}^2 - {k_y}^2), O_3(\vec{k}) = 2k_x k_y$. In the displacement representation, for a 2D square lattice there are two independent variables (u_x, u_y) per lattice point (or per unit cell). In the equivalent (symmetric) strain representation, there are three physical strains e_1, e_2, e_3 and one constraint, so there are again $3 - 1 = 2$ independent variables. We now derive compatibility kernels for transitions with increasing numbers of non-OP strains, $n = 1, 2$.

1. n = 1 cases:

Triangle/center rectangle, square/oblique, and triangle/oblique transitions:

For these three transitions, the two-component OP strain is (e_2, e_3). The single non-OP strain is e_1, and the harmonic term is $\bar{f}_{non} = A_1|e_1|^2$. Substituting from compatibility $e_1 = -\sum_{\ell=2,3} O_\ell e_\ell / O_1$, immediately yields the 2×2 matrix kernel of components[13], with prefactor $\nu(\vec{k})$ inserted, namely $U_{\ell\ell'} = \nu O_\ell O_{\ell'}/{O_1}^2$ so

$$U_{22} = \nu {O_2}^2/{O_1}^2, \ U_{33} = \nu {O_3}^2/{O_1}^2$$

$$U_{23} = \nu O_2 O_3/{O_1}^2 = U_{32}. \ (A2a)$$

Or explicitly,

$$U_{22} = \nu({k_x}^2 - {k_y}^2)^2/k^4, \ U_{33} = \nu(2k_x k_y)^2/k^4$$

$$U_{23} = \nu 2k_x k_y({k_x}^2 - {k_y}^2)/k^4 = U_{32}. \ (A2b)$$

Although these 2D transitions all have $N_{OP} = 2$ and the same compatibility kernel, they of course differ in their Landau or g_L coefficients, and in the different N_V values of their nonzero pseudospin vectors (pointing to corners of a triangle, square, and hexagon, respectively).

2. n = 2 cases:

(a) Square/rectangle transition:

The single OP is the deviatoric strain e_2. The non-OP strains are the 2D compression and shear e_1 and e_3, and the harmonic non-OP free energy is $\bar{f}_{non} = \sum_{i=1,3}(A_i/2)|e_i(\vec{k})|^2$. The compatibility condition yields $e_3 = -\sum_{\alpha=1,2}\bar{O}_\alpha e_\alpha$, where $\bar{O}_\alpha \equiv O_\alpha/O_3$. Substituting yields $\bar{f}_{non} = (A_1/2)[|e_1(\vec{k})|^2 + \sum_{\alpha,\beta=1,2} G_{\alpha,\beta} e_\alpha {e_\beta}^*]$, where $G_{\alpha,\beta} \equiv (A_3/A_1)\bar{O}_\alpha\bar{O}_\beta$.

Freely minimizing in the remaining non-OP variable e_1 as $\partial f_{non}/\partial e_1^*(\vec{k}) = 0$, yields $e_1(\vec{k}) = B_{12}(\vec{k})e_2(\vec{k})$. Substituting back, the local non-OP term $\bar{f}_{non}$ becomes a nonlocal compatibility potential for the OP distortions $\bar{f}_{compat}(e_2) = (A_1/2)U(\vec{k})|e_2(\vec{k})|^2$, where the kernel is

$$U(\vec{k}) = (G_{22} + R_{22,11})/[1 + G_{11}], \quad (A3)$$

where $R_{22,11} \equiv G_{22}G_{11} - {G_{12}}^2$. The structure is similar to the 3D cases below. However, for the 2D case, the remainder term $R_{22,11} = 0$ so this becomes

$$A_1 U(\vec{k}) = \nu {O_2}^2/[\{{O_1}^2/A_1\} + \{{O_3}^2/A_3\}]. \quad (A4a)$$

Or explicitly,

$$A_1 U(\vec{k}) = \nu A_1({k_x}^2 - {k_y}^2)^2/[k^4 + (8A_1/A_3)(k_x k_y)^2]. \quad (A4b)$$

We fix $2A_1/A_3 \simeq 1$ for simplicity, so the strength of the compatibility potential is determined by A_1, that is essentially the elastic anisotropy parameter,[26] by (2.18d). Plots of U have been given elsewhere[11,12]. The same result is obtained through Lagrange multipliers: minimizing $\{f_{non} - \Lambda(\sum_{\alpha=1,2,3} O_\alpha e_\alpha)\}$ in e_1, e_3 yields $e_i = \Lambda O_i/A_i$ for $i = 1, 3$. Demanding compatibility fixes the Lagrange multiplier $\Lambda = -O_2 e_2/[\{O_1^2/A_1\} + \{O_3^2/A_3\}]$, so e_1, e_3 are in terms of e_2, yielding the same kernel (A4).

As mentioned in the text, the square/rhombus is not distinct from the square/rectangle transition. Nonetheless, the OP is now e_3 and the non-OP are e_1, e_2. The kernel is just a $2 \leftrightarrow 3$ label interchange,

$$A_1 U(\vec{k}) = \nu {O_3}^2/(\{{O_1}^2/A_1\} + \{{O_2}^2/A_2\}). \quad (A5)$$

(b) Rectangle/oblique:

The OP is again e_3 but the non-OP energy $\bar{f}_{non} = \sum_{\pm}(A_\pm/2)|e_\pm|^2$ is now harmonic in the combinations $e_+ = \frac{1}{2}(e_1 + e_2)$ and $e_- = \frac{1}{2}(e_1 - e_2)$. The substitution for e_1 through compatibility, and free minimization in e_2 yields the kernel with $O_\pm \equiv O_1 \pm O_2$ as

$$A_1 U(\vec{k}) = \nu {O_3}^2/[\{{O_+}^2/A_+\} + \{{O_-}^2/A_-\}]. \quad (A6)$$

B. 3D transitions

We use the 3D compatibility constraints to obtain St Venant kernels for $n = 3, 4, 5$.

The 3D compatibility conditions of (2.3) in Fourier space for Cartesian distortions $Inc(\mathbf{e}) = \vec{k} \times \mathbf{e}(\vec{k}) \times \vec{k} = 0$, can be written as three equations from diagonal components of Incompatibility, like $Inc(e)_{xx} = 0$,

$$2k_y k_z e_{yz} = k_y^2 e_{zz} + k_z^2 e_{yy};$$

$$2k_z k_x e_{zx} = k_z^2 e_{xx} + k_x^2 e_{zz};$$

$$2k_x k_y e_{xy} = k_x^2 e_{yy} + k_y^2 e_{xx}. \quad (A7)$$

There are also three equations from the off-diagonal components, like $Inc(e)_{yz} = 0$,

$$k_y k_z e_{xx} = -k_x^2 e_{yz} + k_x k_y e_{zx} + k_z k_x e_{xy};$$

$$k_z k_x e_{yy} = -k_y^2 e_{zx} + k_y k_z e_{xy} + k_x k_y e_{yz};$$

$$k_x k_y e_{zz} = -k_z^2 e_{xy} + k_z k_x e_{yz} + k_y k_z e_{zx}, \quad (A8)$$

but these are not new constraints: solving (A7) for shears and substituting, (A8) is satisfied as an identity. In the displacement representation, for a 3D cubic lattice there are three independent variables (u_x, u_y, u_z) per lattice point (or per unit cell). In the equivalent (symmetric) strain representation, there are six physical strains $e_1, .., e_6$ and three constraints, so there are again $6 - 3 = 3$ independent variables.

The 3D St Venant constraints of (A7) in terms of the Cartesian distortions can be written in terms of the cubic-lattice physical distortions (2.6a), by inverting the coefficient matrix, to get

$$e_{xx} = \frac{1}{\sqrt{3}}e_1 + \frac{1}{\sqrt{2}}e_2 + \frac{1}{\sqrt{6}}e_3;$$

$$e_{yy} = \frac{1}{\sqrt{3}}e_1 - \frac{1}{\sqrt{2}}e_2 + \frac{1}{\sqrt{6}}e_3;$$

$$e_{zz} = \frac{1}{\sqrt{3}}e_1 - \frac{2}{\sqrt{6}}e_3. \quad (A9)$$

This yields the 3D St Venant constraints in terms of physical distortions,

$$O_1^{(s)}e_1 + O_2^{(s)}e_2 + O_3^{(s)}e_3 + O_s^{(s)}e_s = 0, \quad (A10)$$

labelled by the three shears, $s = 4, 5, 6$. Defining

$$\bar{O}_\alpha^{(s)} \equiv O_\alpha^{(s)}/O_s, \quad (A11)$$

the shears e_4, e_5, e_6 are related to the non-shears e_1, e_2, e_3 by

$$e_s = -\sum_{\alpha=1,2,3} \bar{O}_\alpha^{(s)} e_\alpha. \quad (A12)$$

The cubic-lattice compatibility coefficients $O_\alpha^{(s)}$ of (A10) are evaluated from (A7) and (A9) as

$$O_1^{(4)} = \frac{-1}{\sqrt{3}}(k_y^2 + k_z^2),\ O_2^{(4)} = \frac{1}{\sqrt{2}} k_z^2;$$

$$O_3^{(4)} = \frac{1}{\sqrt{6}}(2k_y^2 - k_z^2),\ O_4^{(4)} \equiv O_4 = k_y k_z. \ (A13a)$$

$$O_1^{(5)} = \frac{-1}{\sqrt{3}}(k_z^2 + k_x^2),\ O_2^{(5)} = \frac{-1}{\sqrt{2}} k_z^2;$$

$$O_3^{(5)} = \frac{1}{\sqrt{6}}(2k_x^2 - k_z^2),\ O_5^{(5)} \equiv O_5 = k_z k_x. \ (A13b)$$

$$O_1^{(6)} = \frac{-1}{\sqrt{3}}(k_x^2 + k_y^2),\ O_2^{(6)} = \frac{1}{\sqrt{2}}(k_x^2 - k_y^2);$$

$$O_3^{(6)} = \frac{-1}{\sqrt{6}}(k_x^2 + k_y^2),\ O_6^{(6)} \equiv O_6 = k_x k_y. \ (A13c)$$

These will be used in the cubic/tetragonal, cubic/orthorhombic, and cubic/trigonal transitions, below.

For the tetragonal-lattice physical distortions of (2.6b), the Cartesian components can be written as

$$e_{xx} = \frac{1}{\sqrt{2}}(e_1 + e_2);\ e_{yy} = \frac{1}{\sqrt{2}}(e_1 - e_2);\ e_{zz} = e_3, \ (A14)$$

and the tetragonal-lattice compatibility coefficients from (A7) and (A14) are

$$O_1^{(4)} = \frac{-k_z^2}{\sqrt{2}},\ O_2^{(4)} = \frac{k_z^2}{\sqrt{2}},$$

$$O_3^{(4)} = -k_y^2,\ O_4^{(4)} \equiv O_4 = k_y k_z. \ (A15a)$$

$$O_1^{(5)} = \frac{-k_z^2}{\sqrt{2}},\ O_2^{(5)} = \frac{-k_z^2}{\sqrt{2}},$$

$$O_3^{(5)} = -k_x^2,\ O_5^{(5)} \equiv O_5 = k_z k_x. \ (A15b)$$

$$O_1^{(6)} = \frac{-1}{\sqrt{2}}(k_x^2 + k_y^2),\ O_2^{(6)} = \frac{-1}{\sqrt{2}}(k_x^2 - k_y^2),$$

$$O_3^{(6)} = 0, \qquad O_6^{(6)} \equiv O_6 = k_x k_y. \ (A15c)$$

These will be used for the tetragonal/orthorhombic transition, below.

It is useful to define a dimensionless variable, analogous to the 2D version above, namely

$$G_{\alpha\beta} \equiv \sum_{s=4,5,6} (A_s/A_1) \bar{O}_\alpha^{(s)} \bar{O}_\beta^{(s)}, (A16a)$$

where $G_{\alpha\beta} = G_{\beta\alpha}$ is symmetric, and a remainder term as before is defined through products,

$$R_{\alpha\beta,\gamma\delta} = G_{\alpha\beta} G_{\gamma\delta} - G_{\alpha\gamma} G_{\beta\delta}. \ (A16b)$$

Then the kernels for the four 3D transitions are obtained in terms of the $G_{\alpha\beta}$, by a substitution/minimization method similar to 2D.

3. n = 3 case:

Cubic/trigonal transition:

For this transition, the OP strains are the shears $\{e_\ell\} = \{e_s\} = e_4, e_5, e_6$. The non-OP strains are e_1, e_2, e_3, and the harmonic term is $\bar{f}_{non} = \sum_{i=1,2,3} (A_i/2) |e_i(\vec{k})|^2$, with deviatoric coefficients $A_2 = A_3$ by symmetry[16]. Compatibility here gives the shear OP e_4, e_5, e_6 in terms of the non-OP as in (A12), $e_\ell = -\sum_{i=1,2,3} \bar{O}_i^{(s)} e_i$ or in matrix form,

$$\begin{pmatrix} e_4 \\ e_5 \\ e_6 \end{pmatrix} = - \begin{pmatrix} \bar{O}_1^{(4)} & \bar{O}_2^{(4)} & \bar{O}_3^{(4)} \\ \bar{O}_1^{(5)} & \bar{O}_2^{(5)} & \bar{O}_3^{(5)} \\ \bar{O}_1^{(6)} & \bar{O}_2^{(6)} & \bar{O}_3^{(6)} \end{pmatrix} \begin{pmatrix} e_1 \\ e_2 \\ e_3 \end{pmatrix}. \ (A17)$$

The non-OP can be written in terms of the OP shears by inverting the 3×3 coefficient-matrix M above to directly yield $e_i = \sum_{s=4,5,6} B_{is} e_s$. Here $B \equiv M^{-1} = (2/DetM)N$, where $N \equiv adj(M)/2$. The determinant can be written as $DetM/2 = [\bar{O}_1^{(4)} N_{14} + \bar{O}_1^{(5)} N_{15} + \bar{O}_1^{(6)} N_{16}]$. The components N_{is} can be evaluated, such as

$$N_{14} = -\frac{1}{2}[\bar{O}_2^{(5)} \bar{O}_3^{(6)} - \bar{O}_2^{(6)} \bar{O}_3^{(5)}]$$

$$= \frac{1}{2\sqrt{3} O_4}(k_x^2 - k_y^2 - k_z^2). \ (A18)$$

The elements $N_{14}, N_{15}, N_{16}; ...N_{36}$ in matrix form are:

$$\begin{pmatrix} \frac{(k_x^2 - k_y^2 - k_z^2)}{2\sqrt{3}O_4} & \frac{(k_y^2 - k_z^2 - k_x^2)}{2\sqrt{3}O_5} & \frac{(k_z^2 - k_x^2 - k_y^2)}{2\sqrt{3}O_6} \\ \frac{(k_x^2 + k_y^2)}{2\sqrt{2}O_4} & -\frac{(k_x^2 + k_y^2)}{2\sqrt{2}O_5} & -\frac{(k_x^2 - k_y^2)}{2\sqrt{2}O_6} \\ \frac{(2k_z^2 + k_x^2 - k_y^2)}{2\sqrt{6}O_4} & \frac{(2k_z^2 - k_x^2 + k_y^2)}{2\sqrt{6}O_5} & -\frac{(2k_z^2 + k_x^2 + k_y^2)}{2\sqrt{6}O_6} \end{pmatrix}. \ (A19)$$

Evaluation of $DetM$ with (A19) yields the simple result $2/DetM = +1$, so $B_{is} = N_{is}$, and so the non-OP in terms of the OP strains are $e_i = \sum_{s=4,5,6} N_{is} e_s$.

The St Venant compatibility terms are obtained by simple substitution into the non-OP harmonic terms, $\bar{f}_{non} = \sum_{i=1,2,3}(A_i/2)|e_i(\vec{k})|^2 = \sum_{\ell,\ell'=4,5,6}(A_1/2)U_{\ell\ell'}(\vec{k})e_\ell(\vec{k})e_{\ell'}(\vec{k})^*$, where the 3×3 compatibility matrix kernel for the cubic/trigonal transition is

$$A_1 U_{\ell\ell'}(\vec{k}) = \nu \sum_{i=1,2,3} A_i N_{i\ell} N_{i\ell'}, \quad (A20)$$

and can be numerically evaluated in simulations.

4. n = 4 case:

Cubic/ tetragonal and cubic/orthorhombic transitions:

In both cases, the two-component OP are the two $3D$ deviatoric strains (e_3, e_2). The non OP are the remaining compression and shear strains e_1, e_4, e_5, e_6, and their harmonic terms are $\bar{f}_{non} = (A_1/2)|e_1|^2 + \sum_{s=4,5,6}(A_s/2)|e_s(\vec{k})|^2$, with shear coefficients $A_4 = A_5 = A_6$ by symmetry[14,16]. From the compatibility equations (A12), we have $e_s = -\sum_{\alpha=1,2,3} \bar{O}^{(s)}_\alpha e_\alpha$ and hence, using the definition (A16a),

$$\bar{f}_{non} = (A_1/2)[\ |e_1|^2 + \sum_{\alpha,\beta=1,2,3} G_{\alpha,\beta} e_\alpha e_\beta{}^*]. \quad (A21)$$

Minimizing, we get $e_1 = \sum_{\ell=2,3} B_{1\ell} e_\ell$ with $B_{1\ell} = -G_{1\ell}/(1 + G_{11})$ similar in structure to the square/rectangle case. It is easy to check using (A16a) and (A13), that G_{11} depends only on cubic-invariant combinations of k_x, k_y, k_z.

Substituting back into (A21), $f_{non}(e_1) = f_{compat}(e_3, e_2)$ where the St Venant term is

$$\bar{f}_{compat} = \sum_{\ell,\ell'=2,3} (A_1/2) U_{\ell\ell'}(\vec{k}) e_\ell(\vec{k}) e_{\ell'}(\vec{k})^*. \quad (A22)$$

Here, the compatibility kernel for the cubic/tetragonal and the cubic/orthorhombic transitions, is the 2×2 matrix

$$U_{\ell\ell'} = \nu[G_{\ell\ell'} + R_{\ell\ell',11}]/(1 + G_{11}), \quad (A23)$$

with $R_{\ell\ell',11} \equiv G_{\ell\ell'} G_{11} - G_{\ell 1} G_{\ell' 1}$. This kernel can be numerically evaluated in simulations.

As in all cases, the same results can be obtained by minimizing $\{\bar{f}_{non} - \sum_{s=4,5,6} \Lambda^{(s)}[\sum_\alpha O^{(s)}_\alpha e_\alpha]\}$ where there are three Lagrange multipliers $\Lambda^{(s)}$. Then one finds $e_s = \Lambda^{(s)} O_s/A_s$; $e_1 = \sum_s \Lambda^{(s)} O^{(s)}_1/A_1$. From compatibility, $\Lambda^{(s)} = -(A_s/O_s)\sum_{\ell=2,3}[\bar{O}^{(s)}_\ell(1 + G_{11}) - \bar{O}^{(s)}_1 G_{1\ell}]e_\ell/(1 + G_{11})$, yielding the same kernel as before. This kernel was used earlier[13], but is here and in[29] explicitly stated.

5. n = 5 case:

Tetragonal/orthorhombic transition:

For this transition, the single-component OP is one of the deviatoric strains, e_2. The non-OP strains are e_1, e_3, e_4, e_5, e_6, and the harmonic term is $\bar{f}_{non} = (A_1/2)|e_1|^2 + (A_3/2)|e_3|^2 + \sum_{s=4,5,6}(A_s/2)|e_s|^2$, with $A_5 = A_6$ by symmetry[16]. Substituting with (A12), but now with the compatibility coefficients (A15) for the tetragonal case,

$$\bar{f}_{non} = \frac{A_1}{2}[\ \sum_{i=1,3} (A_i/A_1)|e_i|^2 + \sum_{\alpha,\beta=1,2,3} G_{\alpha,\beta} e_\alpha e_\beta{}^*], \quad (A24)$$

where the $G_{\alpha\beta}$ is defined in (A16a).

Minimizing freely in e_1, e_3 and inverting a 2×2 matrix yields

$$e_1 = -[(A_3/A_1)G_{12} + R_{33,12}]e_2/G_0;$$

$$e_3 = -[G_{32} + R_{11,32}]e_2/G_0, \quad (A25a)$$

where $R_{\alpha\alpha,\beta\gamma}$ is defined in (A16b), and

$$G_0 \equiv [(\{A_3/A_1\} + G_{33})(1 + G_{11}) - G^2_{13}]. \quad (A25b)$$

The kernel for the tetragonal/orthorhombic transition is

$$A_1 U(\vec{k}) = \nu[(A_3/A_1)G_{22} + T_2]/G_0, \quad (A26).$$

with $T_2 = (A_3/A_1)R_{22,11} + R_{22,33} + \{G_{22}R_{33,11} - G_{12}R_{33,12} - G_{32}R_{11,32}\}$. The kernel can be evaluated numerically in simulations.

As a check, we take uniformity in the z direction, or $k_z \to 0$, when $O_4, O_5 \to 0$, and it is clear from compatibility that $e_3 = e_4 = e_5 = 0$. Then one recovers, with $4A_6 \to A_3$, precisely the form of the square/rectangle kernel of (A4).

Finally, the compatibility kernels in Fourier space are plotted for the four 3D transitions in Fig. 4 below, reflecting the high temperature unit-cell symmetries.

[1] G.A. Baker, Jr., *Quantitative Theory of Critical Phenomena* (Academic Press, Boston, 1990).

[2] K. Bhattacharyya, *Microstructure of Martensite*, Oxford, U.K., (2003); J.M. Ball and R.D. James, Phil. Trans. Roy. Soc., Lond. A **338**, 389 (1992).

[3] E.K.H. Salje, *Phase Transformations in Ferroelastic and Coelastic Crystals* (Cambridge University Press, Cambridge, U.K., (1990).

[4] V.K. Wadhawan, *Introduction to Ferroic Materials* (Gordon and Breach, New York, 2000).

[5] P. Chaikin and T. Lubensky, *Principles of Condensed Matter Pysics*, L.D. Landau and I.M. Lifshitz, *Elasticity* (Pergamon, 1980).

[6] J.-C. Tolédano and P. Tolédano, *The Landau Theory of Phase Transitions* (World Scientific, Singapore, 1987); J.-C. Tolédano and P. Tolédano, Phys. Rev. B **21**, 1139 (1980); H. T. Stokes and D. M. Hatch, *Isotropy Subgroups of the 230 Crystallographic Space Groups*, World Scientific, Singapore, 1988; K. Aizu, J. Phys. Soc. Jpn. **27**, 387 (1969); J. Sapriel, Phys. Rev. B **12**, 5128 (1975).

[7] S. Vedantam and R. Abeyratne, Int. J. of Nonlinear Mechanics, **40**, 177 (2003); F. Falk and J. Konopka, J. Phys:CM , **2**, 61 (1990).

[8] G.R. Barsch, B. Horowitz, and J.A. Krumhansl, Phys. Rev. Lett. **59**, 1251 (1987); B. Horowitz, G.R. Barsch and J.A. Krumhansl, Phys. Rev. B, **43**, 1021 (1991).

[9] S.F. Borg, *Fundamentals of Engineering Elasticity* (World Scientific, Singapore, 1990); E. Kroener in *Physics of Defects*, ed. R. Balian, M. Kleman and J.P. Pourier, Les Houches session XXV (North Holland, NY, 1980).

[10] M. Baus and R. Lovett, Phys. Rev. Lett. **65**, 1781 (1990); Phys. Rev. A **44**, 1211 (1991).

[11] S. Kartha, J.A. Krumhansl, J.P. Sethna, and L.K. Wickham, Phys. Rev. B **52**, 803 (1995).

[12] S.R. Shenoy, T. Lookman, A. Saxena, and A.R. Bishop, Phys. Rev. B **60**, R12537 (1999).

[13] T. Lookman, S.R. Shenoy, K.Ø. Rasmussen, A. Saxena, and A.R. Bishop, Phys. Rev. B **67**, 02130 (2003).

[14] K.Ø. Rasmussen, T. Lookman, A. Saxena, A.R. Bishop, R.C. Albers, and S.R. Shenoy, Phys. Rev. Lett. **87**, 055704 (2001).

[15] D.M. Hatch, T. Lookman, A. Saxena, and S.R. Shenoy, Phys. Rev. B **68**, 104105 (2003). The program ISOTROPY http://www.physics.byu.edu/~stokesh/isotropy.html by H.T. Stokes and D.M. Hatch generates all symmetry allowed invariants in strain tensor and strain gradient components.

[16] A . Saxena, T. Lookman, A. R. Bishop and S.R. Shenoy, in *Intrinsic multiscale structure and dynamics in complex electronic oxides*, ed. A. R. Bishop, S. Sridhar and S. R. Shenoy, World Scientific, Singapore (2004).

[17] S.R. Shenoy, T. Lookman and A. Saxena, in *Magnetism and Structure in Functional Materials*, ed. A. Planes, L. Manosa and A. Saxena, Springer Verlag, Berlin (2005).

[18] G.R. Barsch and J.A. Krumhansl, Metallurg. Trans. A**18**, 761 (1988): Phys. Rev. Lett., **53**, 1069 (1984); and in *Martensites*, ed. G.B. Olson and W.S. Owen, (ASM International, Materials Park, Ohio, 1992).

[19] J. Tobochnik, Phys. Rev. B **26**, 6201 (1982); R. Savit, Phys. Rev. B **22**, 3443 (1980). M. Blume, Phys. Rev. **141**, 517 (1966); H.W. Capel, Physica (Amsterdam) **32**, 966 (1966).

[20] P.A. Lindgard and O. Mouritsen, Phys. Rev. Lett., **57**, 2458 (1986); A.M. Bratkovsky, S.C. Marais, V. Heine and E.K.H. Salje, J. Phys. Condens. Matter, **6**, 3769 (1994).

[21] E. Vives, J. Goicoechea, J. Ortin and A. Planes, Phys. Rev. E, **52**, R5 (1995).

[22] T. Lookman, S.R. Shenoy and A. Saxena, Bull. Am. Phys. Soc., **49** (1), 1315 (2004).

[23] S.R. Shenoy and T. Lookman, Phys. Rev. B **78**, 144103 (2008).

[24] C. Pariege, H. Zapolsky, and A.G. Khachaturyan, Phys. Rev. B **75**, 054102 (2007); B. Cerruti and E. Vives, Phys. Rev. E **77**, 064114 (2008).

[25] D. Sherrington, J. Phys. Condens. Matter, **20**, 304213 (2008).

[26] R.E. Newnham, *Properties of Materials*, (Oxford University Press, Oxford, 2005), Sections 13.6, and 23.4.

[27] R. Oshima and F. Fujita, Acta Metall. Mater., **4**, 685 (1990); M. Sato, B. Grier, S. Shapiro, H. Miyajima, J. of Physics F, **12**, 2117 (1982); A. Zheludev, S.M. Shapiro, F. Wochner, A. Schwarz, M. Wall and L. Tanner, Phys. Rev. B, **51**, 11310 (1993).

[28] S.H. Curnoe and A.E. Jacobs,Phys. Rev. B **63**, 094110 (2001); Phys. Rev. B, **64**, 064101 (2001); A.E. Jacobs, S.H. Curnoe and R.C. Desai, Phys. Rev. B **68**, 224104 (2003); Y.H. Wen, Y. Wang and L.Q. Chen, Phil. Mag. A **80**, 1967 (2000);

[29] R. Vasseur, T. Lookman, and S.R. Shenoy, Phys. Rev. B (submitted); N. Shankaraiah, K.P.N. Murthy, T. Lookman and S.R. Shenoy, Phys. Rev. Lett. (submitted).

[30] J.M. Ball and R.D. James, Phil. Trans. Roy. Soc., Lond. A **338**, 389 (1992); A.E. Jacobs, Phys. Rev, B **52**, 6327 (1995); B. Muite and O.U. Salman, ESOMAT 2009, 03008 (2009) .

FIG. 1. *Schematic* figures of five distinct ferroelastic transitions driven by strains in 2D, with lower symmetry variants on the right: square to rectangle (SR); rectangle to oblique (RO); triangle to centered-rectangle (TR); square to oblique (SO), triangle to oblique (TO). For the TR case, we mark one of three equivalent lattice-point boxes, that becomes the new centred-rectangle unit cell of the first variant on the right, under the simplest distortion order-parameter. The other two equivalent variants have similar unit-cells, that are simply from $\pm 2\pi/3$ order-parameter rotations of that distortion. For the TO case, the equivalent rotations are integer multiples of $2\pi/6$.

FIG. 2. *Schematic* figures of four ferroelastic transitions in 3D, with the lower symmetry variants on the right: (a) tetragonal to orthorhombic; (b) cubic to tetragonal; (c) cubic to trigonal with two other variants not shown; (d) cubic to orthorhombic with four other variants not shown.

FIG. 3. Scaled free energy versus N_{OP} order parameter components, with minima at austenite zero state and N_V martensite variants, and with arrows to minima denoting pseudospin vectors. (a) Minima on a line for $N_{OP} = 1$, $N_V = 2$, square to rectangle (and also tetragonal to orthorhombic, rectangle to oblique); (b) Minima on a triangle for $N_{OP} = 2$, $N_V = 3$, cubic to tetragonal (and triangle to centered rectangle); (c) Minima on a square for $N_{OP} = 2$, $N_V = 4$, square to oblique polygon; (d) Minima on hexagon for $N_{OP} = 2$, $N_V = 6$, for cubic to orthorhombic (and triangle to oblique); (e) Minima (schematic) on a tetrahedron for $N_{OP} = 3$, $N_V = 8$, cubic to trigonal.

FIG. 4. Compatibility kernel components $U_{\ell,\ell'}(k_x, k_y, k_z)$ in color plots versus (k_x, k_y, k_z) for 3D transitions. (a) Tetragonal to orthorhombic case with $U(\vec{k})$. The strength of the kernel is represented by a color coding in which dark brown represents the relative positive maxima, and dark blue the minima with zero values.The z axis is vertical and the projections shown are at $k_x = 0, k_y = 0$ and $k_z = 0$. The maxima shown appear in the plane $k_y = 0$, and minima for $k_x = 0$ and $k_z = 0$. (b) Cubic to tetragonal (and also cubic to orthorhombic case) kernels, (i) $U_{22}(\vec{k})$, (ii) $U_{33}(\vec{k})$, and (iii) $U_{23}(\vec{k})$. The three components acquire positive values, and assume clover-leaf anisotropy in the 2D planes $k_x = 0, k_y = 0$ and $k_z = 0$. (c) Cubic to trigonal case, with a kernel component $U_{66}(\vec{k})$. In addition to the clover-leaf pattern in the plane $k_y = 0$, there is a butterfly anisotropy in the plane $k_x = 0$, similar to that of the square to rectangle kernel in 2D.

TABLE I. Generic numbers for the scaled Landau free energies, listed in order of increasing number of structural variants N_V. The columns are: (1) the type of transition; (2) spatial dimensionality; (3) order-parameter (OP) dimensionality N_{OP} or number of pseudospin components ; (4) number of free energy minima at transition or number of pseudospin-vector states, $N_V + 1$; (5) maximum-order invariant p_{max} retained in the free energy; (6) number of material coefficients N_{mat}, and type of scaled quasi-universality (q-u) as in text; (7) condition obeyed by OP-space angular location ϕ_m of minima ; (8) 'polyhedron' from minima in N_{OP} dimensions.

Transition	d	N_{OP}	$N_V + 1$	p_{max}	N_{mat}, q-u	angular min condition	polyhedron
tetrag/orthorhombic	3	1	2 +1	6	3, first	$\sin 2\phi_m = 0$	line
square/rectangle	2	1	2 +1	6	3, first	$\sin 2\phi_m = 0$	line
square/ rhombus	2	1	2 +1	6	3, first	$\sin 2\phi_m = 0$	line
rectangle/oblique	2	1	2 +1	6	3, first	$\sin 2\phi_m = 0$	line
cubic/tetragonal	3	2	3 +1	4	3, first	$\sin 3\phi_m = 0$	triangle
triangle/centred rectangle	2	2	3 + 1	4	3, first	$\sin 3\phi_m = 0$	triangle
cubic/trigonal	3	3	4 +1	4	4, second	$\sin 4\phi_m = 0, \cos^2\theta_m = \frac{1}{3}$	tetrahedron
square/oblique	2	2	4 +1	6	4, second	$\sin 4\phi_m = 0$	square
cubic/orthorhombic	3	2	6 +1	8	6, third	$\sin 6\phi_m = 0$	hexagon
triangle/oblique	2	2	6 +1	8	6, third	$\sin 6\phi_m = 0$	hexagon

This figure "figs_Page_01.jpg" is available in "jpg" format from:

http://arxiv.org/ps/1010.5538v2

This figure "figs_Page_03.jpg" is available in "jpg" format from:

http://arxiv.org/ps/1010.5538v2

This figure "figures_Page_04.JPG" is available in "JPG" format from:

http://arxiv.org/ps/1010.5538v2

This figure "figures_Page_05.JPG" is available in "JPG" format from:

http://arxiv.org/ps/1010.5538v2

This figure "figures_Page_07.JPG" is available in "JPG" format from:

http://arxiv.org/ps/1010.5538v2

This figure "figures_Page_08.JPG" is available in "JPG" format from:

http://arxiv.org/ps/1010.5538v2

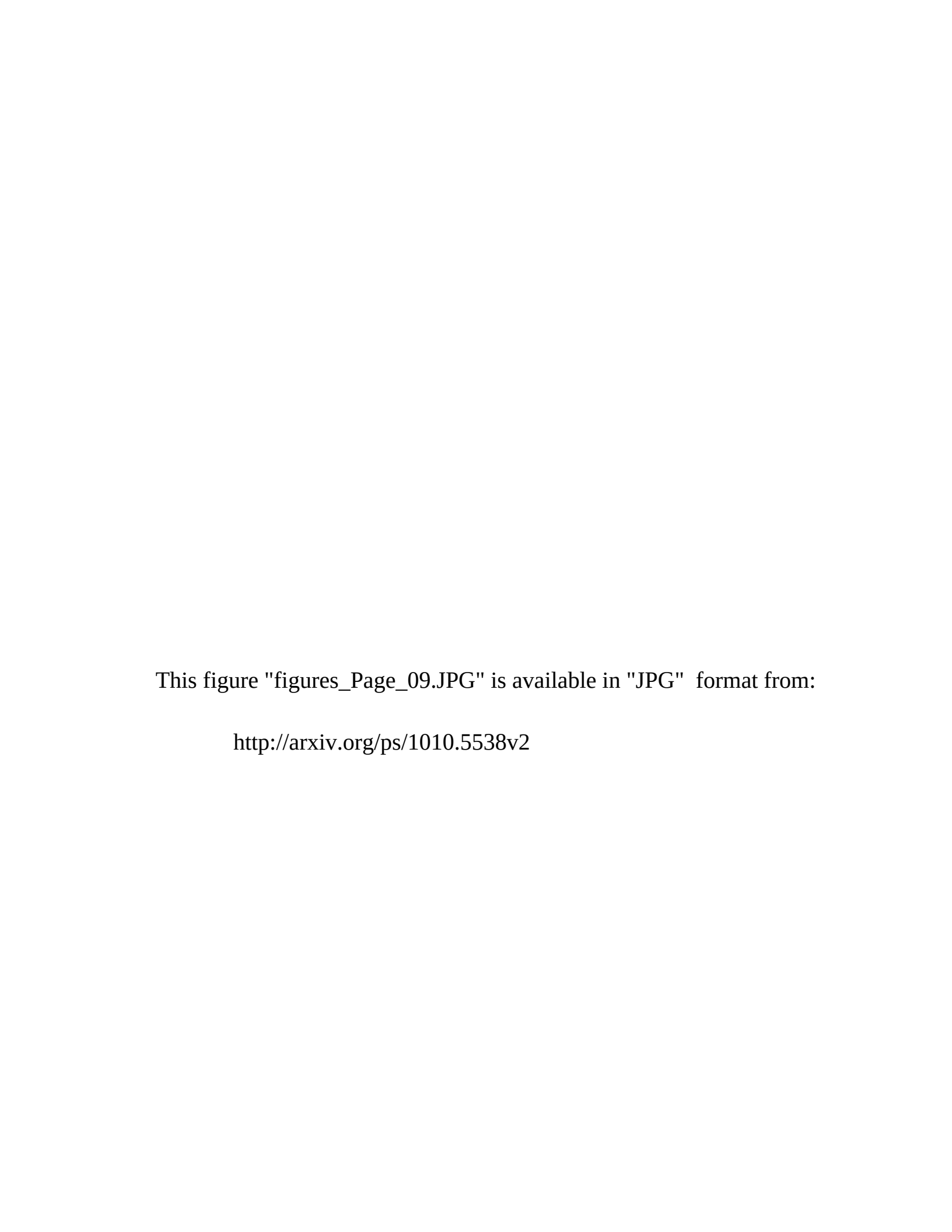
This figure "figures_Page_09.JPG" is available in "JPG" format from:
http://arxiv.org/ps/1010.5538v2

This figure "figures_Page_10.JPG" is available in "JPG" format from:

http://arxiv.org/ps/1010.5538v2

This figure "figures_Page_11.JPG" is available in "JPG" format from:

http://arxiv.org/ps/1010.5538v2